

Discovery of Novel 2,8-Diazaspiro[4.5]decanes as Orally Active Glycoprotein IIb-IIIa Antagonists[†]

Mukund M. Mehrotra,* Julie A. Heath,[§] Mark S. Smyth, Anjali Pandey,[§] Jack W. Rose,[§] Joseph M. Seroogy, Deborah L. Volkots,[§] Lisa Nannizzi-Alaimo,[§] Gary L. Park, Joseph L. Lambing,[§] Stanley J. Hollenbach,[§] and Robert M. Scarborough*[§]

Millennium Pharmaceuticals, Inc., 256 E. Grand Avenue, South San Francisco, California 94080

Received July 25, 2003

In our efforts to develop orally active GPIIb-IIIa antagonists with improved pharmaceutical properties, we have utilized a novel 2,8-diazaspiro[4.5]decane scaffold as a template. We describe here our investigation of a variety of templates including spiropiperidiny- γ -lactams, spiropiperidinylimide, spiropiperidinyureas, and spiropiperidinyhydantoins. With the appropriate acidic and basic pharmacophores in place, each template yielded analogues with potent GPIIb-IIIa inhibitory activity. One of the compounds, **59** (CT50787), was also used to demonstrate for the first time the use of a pharmacological agent which is α IIb β 3 specific to display biological activity in a lower species such as mouse and to extend bleeding times. Evaluation of the pharmacokinetic properties of selected compounds from each series in rat, dog, and cynomolgus monkey has led to the identification of **22** (CT51464), a double prodrug, with excellent pharmacokinetic properties. It exhibited good pharmacokinetic profile across species ($F\% = 33$ (Cyno), 73 (dog), 22 (rat); $t_{1/2\beta} = 14.2$ h (Cyno), 8.97 h (dog), 1.81 h (rat)). The biologically active form, **23** (CT50728), displayed inhibition of platelet aggregation in platelet rich plasma (PRP) with an IC_{50} value of 53 nM in citrate buffer, 110 nM in PPACK anticoagulated PRP, and 4 nM in solid-phase GPIIb-IIIa competition binding assay (ELISA). Both **23** and **22** were stable in human liver microsomes, did not inhibit the P450 3A4 isozyme, and had low protein binding (18.22% for **23**) and a desirable $\log P$ (0.45 ± 0.06 for **22**, and -0.91 ± 0.32 for **23**). It is predicted that the high oral bioavailability for these compounds in multiple species should translate into lower intra- and intersubject variability in man. The long plasma half-life of the lead is consistent with once or twice daily administration for chronic therapy. Analogue **22** (CT51464) thus appears to be a promising oral GPIIb-IIIa inhibitor with significantly improved pharmacokinetic properties over the previously described clinical candidates and may be found useful in the treatment of arterial occlusive disorders.

Introduction

Platelet rich clot formation is important in many vasoocclusive disorders such as unstable angina, acute myocardial infarction, reocclusion after percutaneous interventions, and stroke.¹ Platelet activation is produced by a wide variety of stimuli, but the final common event leading to platelet rich thrombus formation is the binding of the activated platelet integrin GPIIb-IIIa² to the soluble plasma adhesive proteins fibrinogen (Fg) and von Willebrand factor (vWf).³ Fibrinogen and von Willebrand factor are multivalent and participate in the aggregation of platelets to form thrombi at the site of atherosclerotic plaque rupture. If GPIIb-IIIa is blocked from binding to adhesive proteins, then it should prevent formation and/or propagation of a platelet thrombus, no matter what the physiological stimuli was that initiated GPIIb-IIIa activation.⁴ The use of intravenous GPIIb-IIIa inhibitors (eptifibatide, tirofiban, abciximab) in preventing vessel closure after percutaneous coronary angioplasty (PTCA) is now well estab-

lished,⁵ and GPIIb-IIIa receptor antagonists are considered to be the most potent antiplatelet drugs available to the clinician.

Since chronic oral administration of GPIIb-IIIa antagonists could potentially address the additional indications of myocardial infarction and stroke, two of the most deadly cardiovascular diseases in the Western World, intense efforts have been devoted to the discovery of orally active GPIIb-IIIa antagonists.^{6–9} Unfortunately, despite the success of intravenous anti-platelet GPIIb-IIIa antagonists (ReoPro, Integrilin, and Aggrastat)^{5,10} in preventing cardiac events in the hospital, several clinical trials involving oral formulations of “super-aspirins” have failed to show prophylactic benefit in patients with recurrent vascular events in a long term dosing environment. Efficacy analysis of the oral agents orbofiban, xemilofiban, sibrafiban, and lotrafiban (Figure 1)^{8,9,11} in the presence or absence of background aspirin showed no benefit to the composite endpoint of death, recurrent myocardial infarction, and other recurrent ischemic events. Overall, the results have been quite disappointing. Long-term oral GPIIb-IIIa inhibition has uniformly failed to provide protection from ischemic events and was associated with a paradoxical increase in adverse events. Mortality increased in each of the five trials (EXCITE, OPUS-TIMI 16, BRAVO,

* To whom correspondence should be addressed. M.M.: Tel: 650-866-4847. E-mail: mukund_mehrotra@hotmail.com. R.S.: Tel: 650-246-7444. Fax: 650-615-9023. E-mail: rscarborough@portola.com.

[†] Dedicated to Professor E. J. Corey on the occasion of his 75th birthday.

[§] Current address: Portola Pharmaceuticals, Inc., 270 E. Grand Ave, Suite 22, South San Francisco, CA, 94080.

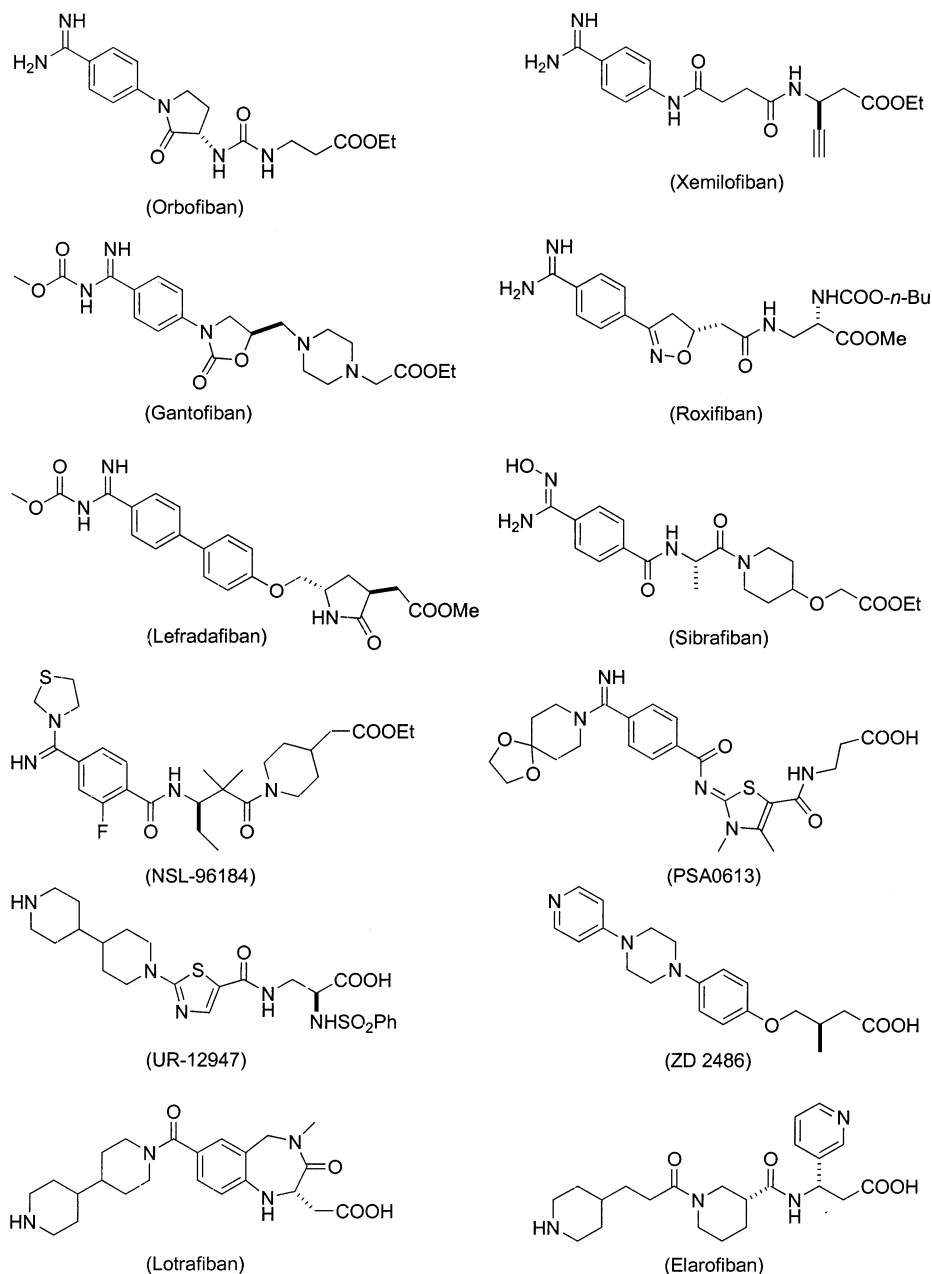


Figure 1. Oral GPIIb/IIIa antagonists that have been studied in advanced stage clinical trials.

SYMPHONY, 2nd SYMPHONY). A combined analysis reveals a highly significant 35% relative (or 0.7% absolute) increase in the risk of death in the 45 523 patients studied, with a 2-fold increase in the risk of bleeding.^{9b}

Many reasons for the failure of orally administered GPIIb-IIIa inhibitors to prevent recurrent cardiac events have been proposed.^{4,12,13} One leading explanation is that the pharmacokinetic properties of the agents tested so far were suboptimal. Short half-lives of these agents can result in large peak-to-trough ratios and poor oral bioavailability can result in significant intra- and interindividual variability of drug in the blood stream of individual patients. Either excess or insufficient drug in the bloodstream at any given time point may lead to undesirable consequences. Excessive drug levels may prevent the blood from clotting when necessary, such that bleeding events result. Too little drug may be ineffective in preventing the platelet aggregation that

leads to cardiac events. It has also been suggested that GPIIb-IIIa inhibitors may lead to platelet activation and/or to the release of inflammatory mediators, at least under certain conditions or at specific drug concentrations.^{13b} The proinflammatory trigger of subthreshold receptor blockade, particularly in the setting of high arterial shear stress, could be quite eventful. It is possible that improved pharmacokinetic properties would therefore lead to a successful oral GPIIb-IIIa inhibitor drug. Other potential mechanisms by which these drugs may cause the undesired side effects are also under investigation. While an in-depth biological examination of this class of antiplatelet drugs is needed, studies until recently have continued on two oral GPIIb-IIIa inhibitors, roxifiban and cromafiban, which have different properties from the earlier oral agents.^{9a,12,14}

The key aim of our investigation has been to identify active and selective GPIIb-IIIa inhibitors with improved pharmacokinetic properties. Most synthetic efforts in

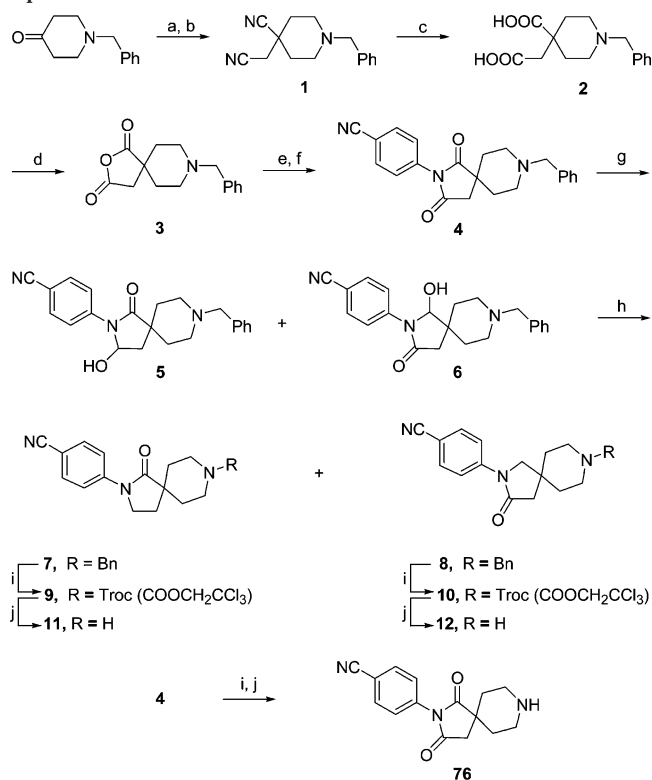
the GPIIb-IIIa inhibitor class have focused on developing novel templates upon which an acidic and a basic pharmacophore are appended. Many classes of GPIIb-IIIa antagonists have been reported which contain constrained templates consisting of monocyclic and/or fused bicyclic scaffolds.¹¹ We have previously reported the use of spirocyclic scaffolds for designing potent GPIIb-IIIa antagonists.¹⁵ Herein, we describe the optimization of the novel 2,8-diazaspiro[4.5]decane scaffold for obtaining orally active and selective inhibitors. Within this spirocyclic framework, highly potent compounds were obtained with favorable pharmacokinetics in the spiro lactam, spirohydantoin, and spirourea templates. The spiro lactam series which has a carbonyl group adjacent to the spiro ring junction (1-oxo) exhibits the most favorable pharmacokinetic profiles. Optimized compounds were evaluated for efficacy and pharmacokinetics in rat, dog, and cynomolgus monkey. Synthesis, SAR, and pharmacokinetics of these compounds are described leading to the identification of the optimized prodrug analogue **22** (CT51464).

Chemistry

For the synthesis of the proposed compounds, we first prepared the diazaspino benzonitrile scaffolds (**11**, **12**, **18a**, **18b**, **19a**, **19b**, and **76**), followed by elaboration into the final targets. The spiro piperidines were first coupled with various carboxy-containing appendages, followed by transformation of the benzonitrile functionality into the corresponding benzamides.¹⁶

The synthesis of the γ -spiro lactams, 4-(1-oxo-2,8-diazaspiro[4.5]dec-2-yl)benzonitrile **11**, 4-(3-oxo-2,8-diazaspiro[4.5]dec-2-yl)benzonitrile **12**, and spiroimide, 4-(1,3-dioxo-2,8-diazaspiro[4.5]dec-2-yl)benzonitrile **76**, are described in Scheme 1. Starting from the commercially available 1-benzyl-4-piperidone, the two γ -lactam scaffolds were synthesized in 10 steps in an overall yield of 22%. 1-Benzyl-4-piperidone was first subjected to Knoevenagel condensation with ethyl cyanoacetate, followed by reaction of the α,β -unsaturated ester with KCN to give the dinitrile **1**. This was hydrolyzed with concentrated HCl to yield the diacid **2**, which was subsequently dehydrated with DCC to furnish the anhydride **3**. The anhydride was reacted with 4-cyanoaniline to yield the mixture of amide-carboxylic acids, which were cyclized with NaOAc/Ac₂O to give the imide **4**. The imide was reduced nonselectively with NaBH₄ in methanol to give a mixture of hydroxy-spiro lactams **5** and **6**, which were reduced with NaBH₄/TFA to give a mixture of the spiro lactams **7** and **8** (ca. 1:2 by NMR, and analytical HPLC, vide infra). This mixture of isomeric lactams proved difficult to separate by flash chromatography on large scale, and so it was used in the next step without purification. The *N*-benzyl group was then conveniently deprotected in two steps as follows. Reaction with 2,2,2-trichloroethyl chloroformate (TrOCOCI) brought about the protective group exchange to yield trichloroethyl-carbamates **9** and **10**.¹⁷ This mixture of Troc-lactams was more easily separable by silica gel chromatography, and at this step both the lactams were fully characterized (¹H NMR). The carbamates **9** and **10** were then individually treated with 10% Cd–Pb couple to effect reductive cleavage¹⁸ of the Troc group to give the key γ -spiro lactam intermediates

Scheme 1^a Synthesis of the γ -Spiro lactam Scaffolds: 4-(1-Oxo-2,8-Diazaspiro[4.5]dec-2-yl)benzonitrile **11**, 4-(3-Oxo-2,8-diazaspiro[4.5]dec-2-yl)benzonitrile **12**, and Spiroimide Scaffold **76**



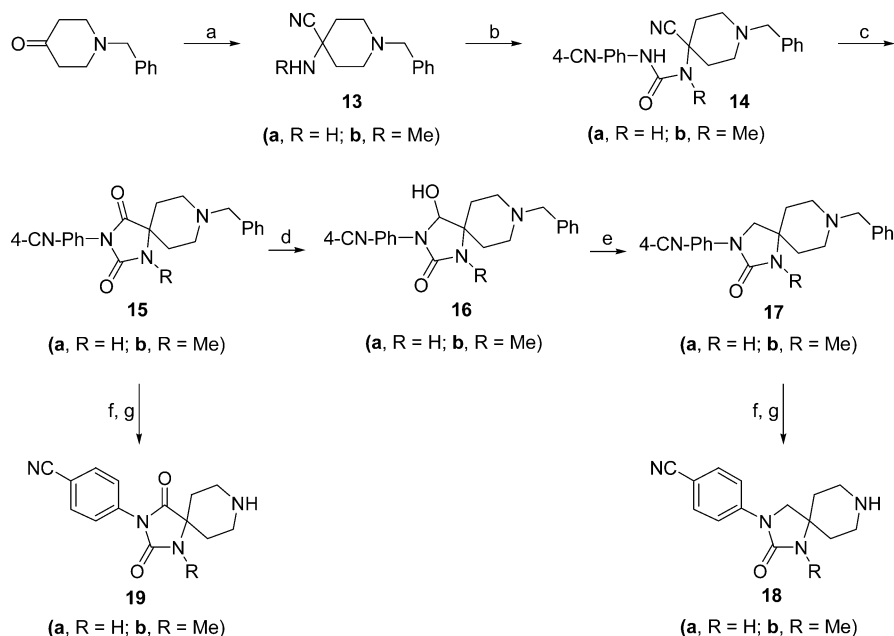
^a Reagents and conditions: (a) ethyl cyanoacetate, Et₃N, CH₂Cl₂, 4 Å sieves; (b) KCN, EtOH/H₂O, Δ; (c) concd HCl, Δ; (d) DCC, DMF; (e) 4-cyanoaniline, TEA, DMF, rt; (f) Ac₂O, NaOAc, Δ; (g) NaBH₄, MeOH; (h) NaBH₄, TFA; (i) 2,2,2-trichloroethyl chloroformate, CH₃CN/CH₂Cl₂; separate isomers by flash chromatography; (j) 10% Cd–Pb, THF/NH₄OAc, pH = 5.

11 and **12**, respectively. This high yielding *N*-debenzylation route was also used for the conversion of **4** to afford the spiroimide **76**.

The synthesis of spirohydantoin, 4-(1-methyl-2,4-dioxo-1,3,8-triazaspiro[4.5]dec-3-yl)benzonitrile (and its 1-H analogue) **19b,a**, and of the spiroureas, 4-(1-methyl-2-oxo-1,3,8-triazaspiro[4.5]dec-3-yl)benzonitrile (and its 1-H analogue) **18b,a**, are described in Scheme 2.¹⁹ 1-Benzyl-4-piperidone was subjected to Strecker conditions by reaction with KCN and either ammonium chloride or methylamine hydrochloride to give α -aminonitriles **13a** and **13b**, respectively. These were then coupled with 4-cyanophenyl isocyanate to yield α -urea nitriles **14**. Cyclization to hydantoin **15** was effected by treatment with 1 N HCl at reflux. The *N*-benzyl group was then removed as described before to afford the spirohydantoin scaffolds **19a,b**. For the synthesis of the spirourea template, the hydantoin **15** was first reduced with NaBH₄/MeOH to give the hydroxy-urea intermediates **16**, followed by treatment with NaBH₄/TFA as described previously to yield **17**. *N*-Debenzylation provided the key intermediates **18a,b**.

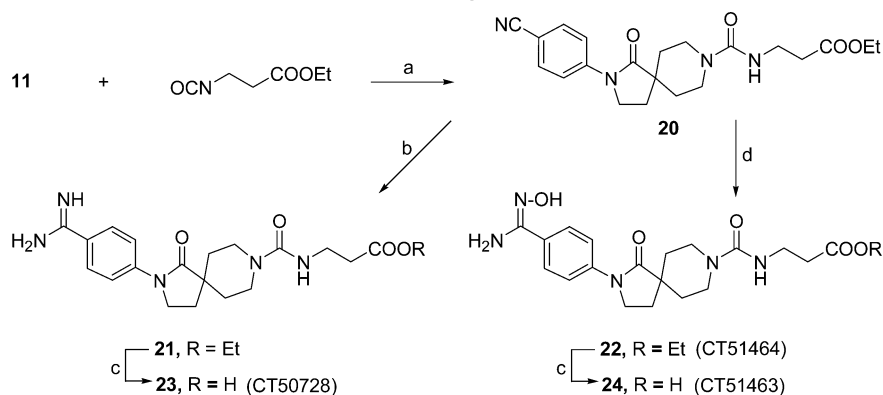
The spiro piperidines (**11**, **12**, **18a,b**, **19a,b**, and **76**) were coupled with the carboxy-containing appendages by standard methods (Schemes 3–15). The required carboxylic acids, acid chlorides, and isocyanates were either commercially available or were synthesized as shown (Schemes 5, 7–13, and 15).

Scheme 2^a Synthesis of the Hydantoin and the Urea Scaffolds: 4-(1-Methyl-2,4-dioxo-1,3,8-triazaspiro[4.5]dec-3-yl)benzotrile (and its 1-H analog) **19b,a** and 4-(1-Methyl-2-oxo-1,3,8-triazaspiro[4.5]dec-3-yl)benzotrile (and its 1-H analog) **18b,a**



^a Reagents and conditions: (a) KCN, RNH₂·HCl, EtOH/H₂O; (b) 4-cyanophenyl isocyanate, Et₃N, CH₂Cl₂; (c) 1 N HCl, Δ; (d) NaBH₄, MeOH; (e) NaBH₄, TFA; (f) 2,2,2-trichloroethyl chloroformate, CH₃CN/CHCl₃; (g) 10% Cd-Pb, THF/NH₄OAc, pH = 5.

Scheme 3^a Synthesis of **23** (CT50728) and Its Double Prodrug **22** (CT51464)



^a Reagents and conditions: (a) CH₂Cl₂, Et₃N, rt.; (b) (i) H₂S, pyridine/Et₃N; (ii) CH₃I, acetone; (iii) NH₄OAc, MeOH; (c) 1 M LiOH, THF, rt; or 3 N HCl, rt; (d) NH₂OH·HCl, Et₃N, EtOH, rt.

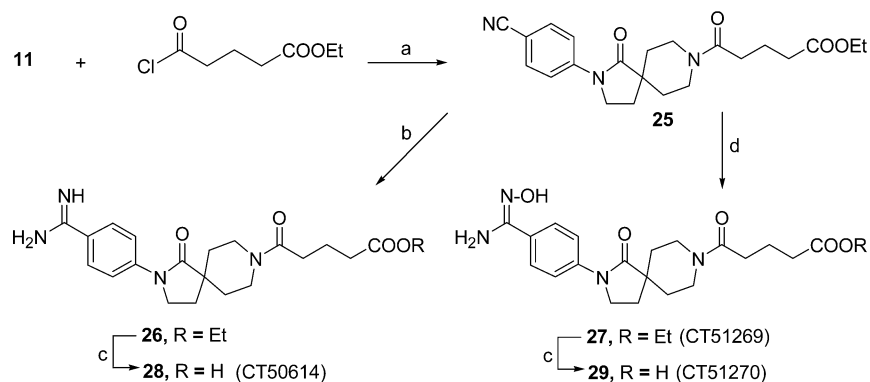
The general synthesis of the compounds with 3-urea-propionic acid tails (e.g., **23**) and their double prodrugs (e.g., **22**) is described in Scheme 3. The spiro-piperidines were reacted with ethyl 3-isocyanatopropionate to give rise to the coupled urea compounds. The benzonitrile functionality was then converted into amidine either via thio-Pinner reaction^{16a} or via amidoximes.^{16b} Reaction of the benzonitriles with hydroxylamine hydrochloride/Et₃N yielded the amidoxime ethyl ester double prodrugs. An analogous scheme for the synthesis of the corresponding amide-linked compounds, 5-oxo-5-azaspiro-1-yl-pentanoic acids (e.g., **28**), is described in Scheme 4. The spiro-piperidines were first reacted with ethyl succinyl chloride, followed by transformation of the benzonitriles into benzamides.

Scheme 5 depicts the synthesis of the oxy-acetic acid analogue **33** and its amidoxime ethyl ester double prodrug **36**. Benzyl glycolate was subjected to a carbene insertion reaction with *tert*-butyl diazoacetate under rhodium(II) acetate dimer catalysis to yield **30a**. The

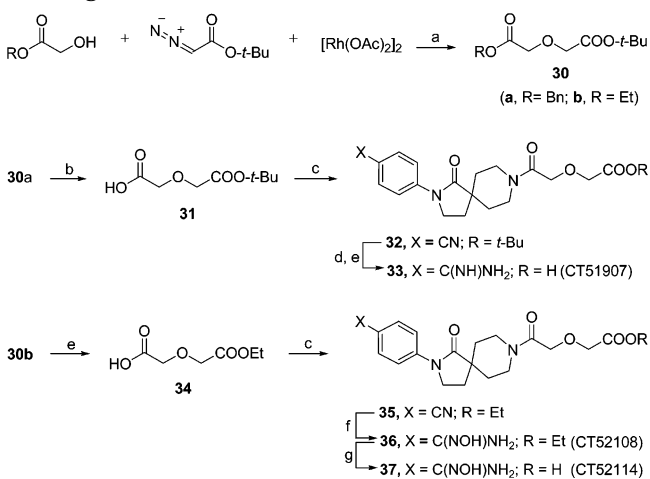
benzyl group was then hydrogenolyzed to yield acid **31**, which was subsequently coupled with spiro-lactam **11** to afford **32**. The benzonitrile function was then transformed into **33** and **36** as described before.

Scheme 6 depicts the synthesis of the substituted amidine analogues **39b** and **40b**. The benzonitrile **25** was converted to thiomethylimidate **38** by the thio-Pinner procedure. Thiomethylimidate **38** was then treated with a mixture of morpholine and acetic acid (ca. 1:2) in methanol to afford **39a**. When acetic acid was omitted a poor yield of **39a** was obtained and the major byproduct was the starting nitrile **25**, formed via the base-catalyzed elimination of CH₃SH from **38**. The same protocol was used for the synthesis of the *N*-ethylamidine analogue **40a**. Treatment of **39a** and **40a** with 3 N HCl yielded **39b** and **40b**.

The synthesis of **44** and **45**, the 3-(*S*)-methyl and 3-(*R*)-methyl analogues of **28**, were achieved by using the route described in Scheme 7. (*R*)-1-Ethyl hydrogen 3-methylglutarate was converted to its *tert*-butyl ester

Scheme 4^a Synthesis of **28** (CT50614) and Its Double Prodrug **27** (CT51269)

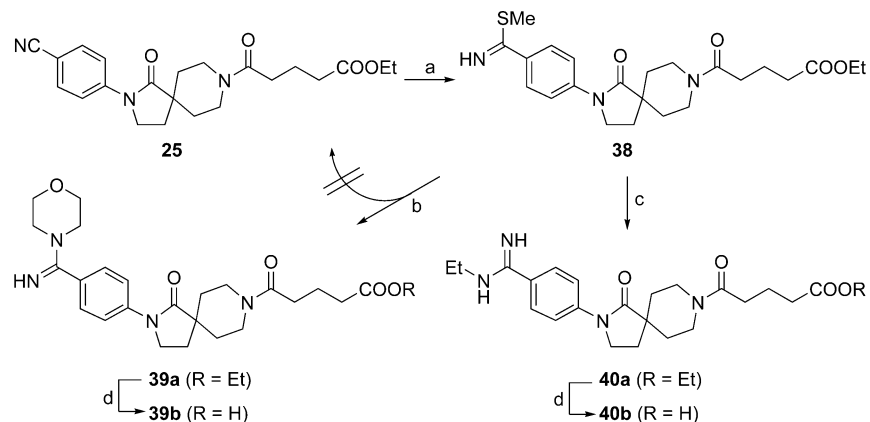
^a Reagents and conditions: (a) DMF, DIEA, rt.; (b) (i) H₂S, pyridine/Et₃N; (ii) CH₃I, acetone; (iii) NH₄OAc, MeOH; (c) 3 N HCl, rt.; (d) NH₂OH·HCl, Et₃N, EtOH, rt.

Scheme 5^a Synthesis of **33** (CT51907) and Its Double Prodrug **36** (CT52108)

^a Reagents and conditions: (a) CH₂Cl₂, rt.; (b) Pearlman's catalyst, EtOAc, 40 psi H₂; (c) **11**, HBTU, DIEA, DMF; (d) (i) H₂S, Pyr/Et₃N; (ii) CH₃I, acetone; (iii) NH₄OAc, MeOH; (e) TFA; (f) NH₂OH·HCl, Et₃N, EtOH; (g) 3 N HCl.

derivative **41**. The ethyl ester was then saponified to give free acid **42**. This was coupled with spirolactam **11** to yield the benzonitrile intermediate **43**, which was then transformed to **44** as described previously. A similar sequence of reactions provided the (*R*)-isomer **45**.

Scheme 8 describes the synthesis of **48**, which is the 3-phenyl-substituted analogue of **28**. 3-Phenylglutaric

Scheme 6^a Synthesis of the Substituted Amidine Analogues **39b** and **40b**

^a Reagents and conditions: (a) (i) H₂S, pyridine/Et₃N; (ii) CH₃I, acetone; (b) morpholine, AcOH, MeOH, rt.; (c) EtNH₂, AcOH, MeOH, rt.; (d) 3 N HCl, rt.

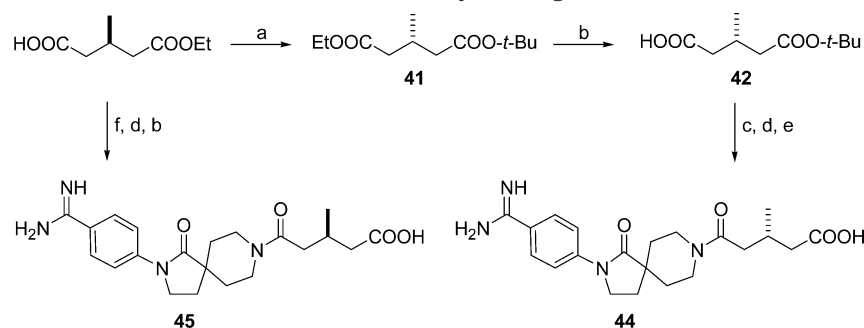
acid was converted to 3-phenylglutaric anhydride by refluxing in acetic anhydride. This was then reacted with EtOH/Et₃N to yield **46**, which was carried forward to **48** by procedures described before.

The synthesis of **53**, the 3-(*S*)-methyl analogue of **23**, is shown in Scheme 9. Cbz-*D*-Alanine was subjected to Arndt–Eistert homologation conditions to yield **49**.^{23b} This was debenzylated to give ethyl (*S*)-3-aminobutanoate **50**, which was then converted to its 4-nitrophenyl carbamate derivative **51**. The carbamate was reacted with the spirolactam **11** to yield **52**, which was then transformed to **53** as described previously.

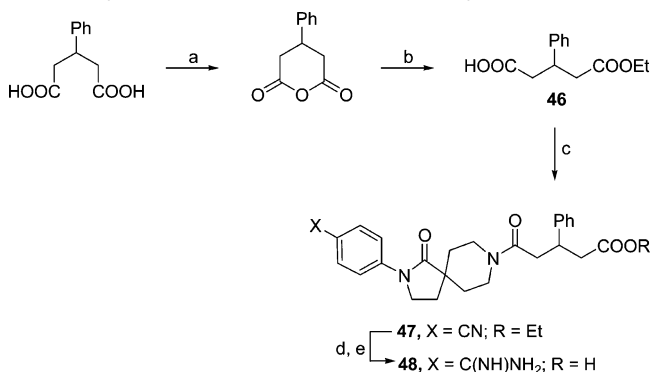
Scheme 10 describes the synthesis of spirohydantoin analogue **56**. Ethyl 3-amino-3-phenylpropanoate was reacted with 4-nitrophenyl chloroformate to yield the 4-nitrophenyl carbamate derivative **54**. This was then reacted with **19b** to afford **55**, which was carried through to **56** as described previously.

Scheme 11 depicts the synthesis of **59**, the 2-*R*-(3,5-dimethylisoxazole-4-sulfonamide) analogue of **28**. H-Glu-*O-t*Bu was reacted with 3,5-dimethylisoxazole-4-sulfonyl chloride under Schotten–Baumann conditions to afford the sulfonamide **57**. This was coupled with spirolactam **11** to yield **58**, which was converted to **59** as described before.

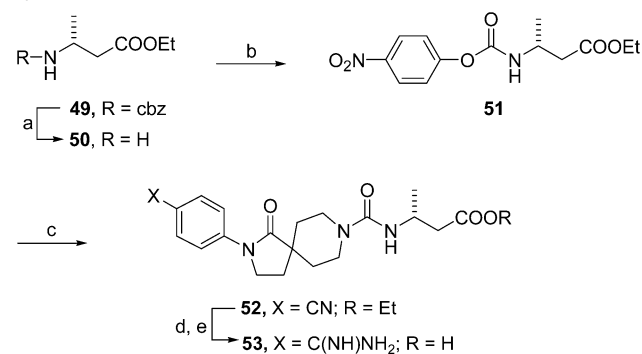
Scheme 12 describes the synthesis of **63**, the α -tosylamide analogue of **23**. Ethyl (*S*)-2-amino-3-(Boc-amino)propanoate was reacted with TsCl to yield tosylamide **60**. Treatment with TFA yielded amine **61**. This was

Scheme 7^a Synthesis of **44** and **45**, the 3-(*S*)- and 3-(*R*)-Methyl Analogues of **28**

^a Reagents and conditions: (a) DCC, *t*-BuOH, CH₂Cl₂; (b) 1 M LiOH, THF; then AcOH; (c) **11**, HBTU, DIEA, DMF → **43**; (d) (i) H₂S, Pyr/Et₃N; (ii) CH₃I, acetone; (iii) NH₄OAc, MeOH; (e) TFA; (f) **11**, EDC·HCl, HOBT, DMF.

Scheme 8^a Synthesis of the 3-Phenylpentanedioic Acid Monoethyl Ester **46** and Its Use in the Synthesis of **48**

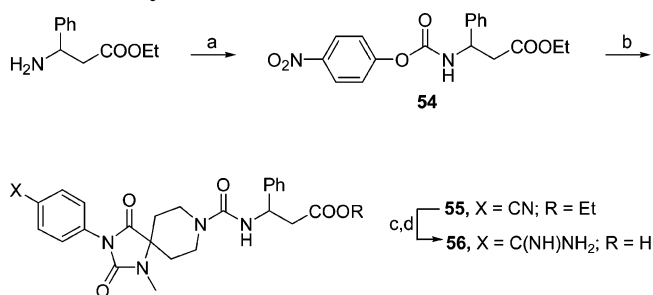
^a Reagents and conditions: (a) Ac₂O, Δ; (b) EtOH, Et₃N, Δ; (c) **11**, EDC·HCl, HOBT, DMF; (d) (i) H₂S, Pyr/Et₃N; (ii) CH₃I, acetone; (iii) NH₄OAc, MeOH; (e) 1 M LiOH, THF/H₂O.

Scheme 9^a Synthesis of the 3-(4-Nitrophenoxycarbonylamino)butyric Acid Ethyl Ester **51** and Its Use in the Synthesis of **53**

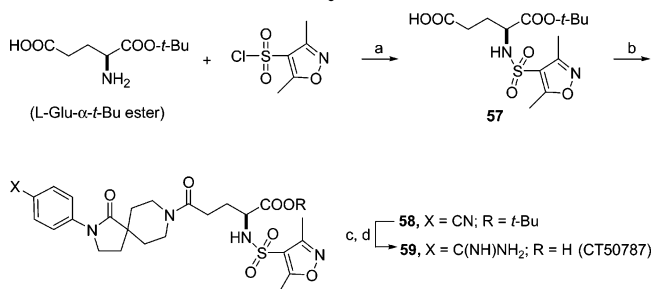
^a Reagents and conditions: (a) 20% Pd(OH)₂/C, EtOAc, 50 psi H₂; (b) 4-nitrophenyl chloroformate, DIEA, CH₂Cl₂; (c) **11**, DIEA, CH₂Cl₂; (d) (i) H₂S, Pyr/Et₃N; (ii) CH₃I, acetone; (iii) NH₄OAc, MeOH; (e) 3 N HCl.

then reacted with triphosgene, followed by spiroactam **11** to give **62**. The benzonitrile functionality was converted to the amidine via the amidoxime route. **62** was reacted with hydroxylamine hydrochloride/Et₃N to yield the amidoxime, which was O-acetylated with Ac₂O/AcOH, and then hydrogenolyzed to yield benzamidine. Hydrolysis of the ethyl ester with 1 M LiOH then provided **63**.

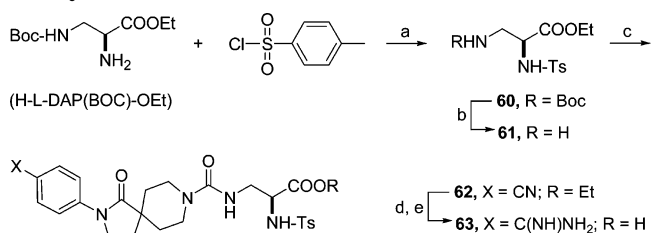
The synthesis of **69**, the α -*n*-butyl carbamate analogue of **28**, was achieved by the route outlined in Scheme 13. Z-Glu(O-*t*-Bu)-OH was converted to its ethyl ester **64**, followed by deprotection of the Cbz-group to

Scheme 10^a Synthesis of the 3-(4-Nitrophenoxycarbonylamino)-3-phenylpropionic Acid Ethyl Ester **54** and Its Use in the Synthesis of **56**

^a Reagents and conditions: (a) 4-nitrophenyl chloroformate, DIEA, CH₂Cl₂; (b) **19b**, DIEA, CH₂Cl₂; (c) (i) H₂S, Pyr/Et₃N; (ii) CH₃I, acetone; (iii) NH₄OAc, MeOH; (d) 1 N LiOH, THF/H₂O.

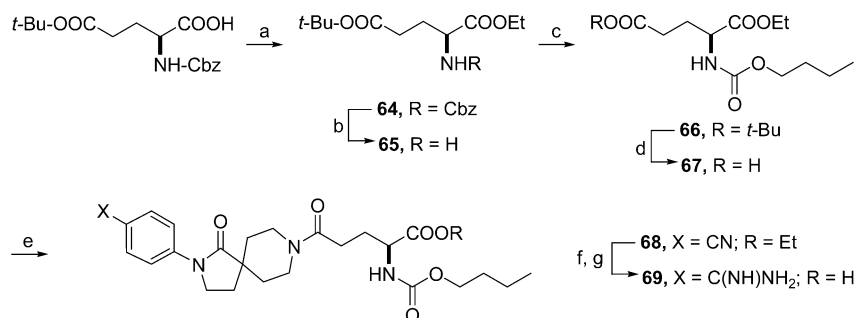
Scheme 11^a Synthesis of the 2-(2-Carboxyethyl)-2-(3,5-dimethylisoxazole-4-sulfonylamino)-3,3-dimethylbutyric Acid **57** and its Use in the Synthesis of **59** (CT50787)

^a Reagents and conditions: (a) (i) 1 N NaOH, Na₂CO₃, 0 °C; (ii) 2 N HCl to pH = 3; (b) **11**, EDC·HCl, DMF; (c) TFA; (d) (i) H₂S, Pyr/Et₃N; (ii) CH₃I, acetone; (iii) NH₄OAc, MeOH.

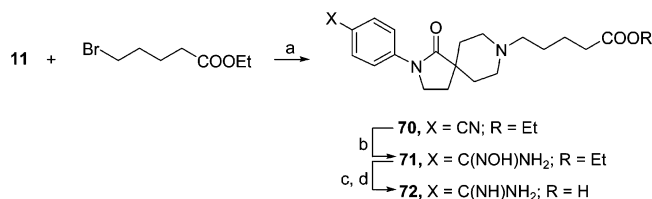
Scheme 12^a Synthesis of the 3-Amino-2-(toluene-4-sulfonylamino)propionic Acid Ethyl Ester **61** and its Use in the Synthesis of **63**

^a Reagents and conditions: (a) DIEA, DCM; (b) TFA; (c) **11**, triphosgene, CH₂Cl₂; (d) (i) NH₂OH·HCl, Et₃N, EtOH; (ii) Ac₂O, AcOH; (iii) 10% Pd/C, H₂, 40 psi; (e) 1 M LiOH, THF/H₂O.

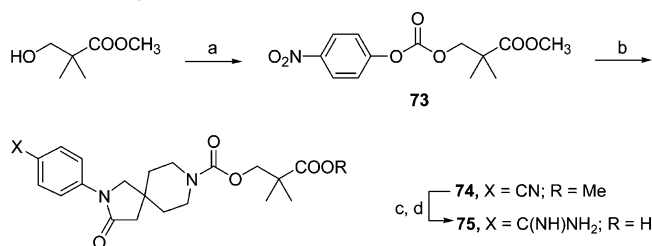
yield **65**. This was reacted with *n*-butyl chloroformate to yield the carbamate **66**. De-*tert*-butylation gave **67**. This was then coupled with the spiroactam **11** to yield

Scheme 13^a Synthesis of the 2-Butoxycarbonylamino-pentanedioic Acid 1-Ethyl Ester **67** and Its Use in the Synthesis of **69**

^a Reagents and conditions: (a) EDC·HCl, HOBT, EtOH, DMF; (b) 20% Pd(OH)₂/C, 1 atm H₂, EtOH; (c) *n*-butyl chloroformate, DIEA, CH₂Cl₂; (d) TFA; (e) **11**, HBTU, DIEA, DMF; (f) (i) NH₂OH·HCl, Et₃N, EtOH; (ii) Ac₂O, AcOH; (iii) 10% Pd/C, 1 atm H₂; (g) 1 M LiOH, THF/H₂O.

Scheme 14^a Synthesis of the 5-Azaspiro-1-ylpentanoic Acid Analogue **72**

^a Reagents and conditions: (a) DIEA, DMF, rt.; (b) NH₂OH·HCl, Et₃N, EtOH; (c) (i) Ac₂O, AcOH; (ii) 10% Pd/C; H₂, 40 psi; (d) 1 N LiOH, THF/H₂O, rt.

Scheme 15^a Synthesis of the 2,2-Dimethylpropionic Acid Analogue **75**

^a Reagents and conditions: (a) 4-nitrophenyl chloroformate, DIEA, CH₂Cl₂; (b) **12**, DIEA, DMF; (c) (i) H₂S, Pyr/Et₃N; (ii) CH₃I, acetone; (iii) NH₄OAc, MeOH; (d) 1 N LiOH, THF/H₂O.

68 and converted to **69** using previously described procedures.

Scheme 14 describes the synthesis of **72**, which is the amine analogue of amide **28**. The spirocyclic lactam **11** was alkylated with ethyl 5-bromovalerate to yield **70**. The benzimidazole functionality was converted to benzamidine via amidoxime **71**, and then the ester group was saponified to yield **72**.

In Scheme 15 is outlined the synthesis of **75**. Methyl 2,2-dimethyl-3-hydroxypropionate was reacted with 4-nitrophenyl chloroformate to yield **73**. This was coupled with spirocyclic amide **12** to give **74**, which was converted to **75** by previously described procedures.

All the final compounds were purified by RP-HPLC and isolated either as their trifluoroacetate or HCl salts.

Results and Discussion

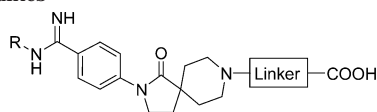
In Vitro SAR. On the basis of our previous studies with other spirocyclic scaffolds,¹⁵ initially the SAR investigation focused on optimizing the distance between the basic amidine functionality and the carboxylic acid group. This bond distance has been hypothesized

to mimic the spacing between the basic guanidine and the acidic carboxylate of the RGD sequence of fibrinogen, which has been approximated to be 10–20 Å.²⁰ To explore this, we synthesized amides with C₂ to C₅ linkers (Table 1; **77**, **78**, **28**, **79**). The C₄-linker was found to be optimum (**28**). By comparison, the compound with C₃-linker (**78**) was found to be 9 times less potent, and the longer version with a C₅-linker (**79**) was about 42 times less potent. This four-atom spacing between piperidine and carboxylate was found to be optimal in all the spiro-templates reported herein.

The potent activity of compound **28** confirmed to us that this novel series merited further investigation. The compounds of Table 1 were prepared to explore the SAR of this 1-oxo- γ -spirocyclic lactam series. In essence, having worked out the crucial spacing between the essential acidic and basic pharmacophores, we undertook the synthesis of numerous analogues of compound **28** to optimize its potency and improve *in vivo* properties.

On the basis of our previous observations^{20,21} as well as those reported in the literature for other series of integrin inhibitors, we targeted two regions of the lead molecule **28** for modification: the central rigid [4.5]-spirocyclic nucleus and the carboxyl linker unit. In the spirocyclic nucleus, we investigated the isomeric 3-oxo- γ -spirocyclic lactam, spirocyclic imide, spirocyclic ureas, and spirocyclic hydantoin. On the linker unit, we compared urea with amide linkages to the piperidine of the scaffold and we made substitutions α or β to the carboxylate terminus.

Most of the compounds in which the carboxylic acid appendage is attached to the piperidine via a urea linkage are generally slightly more potent than the corresponding amides (**28** versus **23** (Table 1); **87** versus **84** (Table 2); **94** versus **89** (Table 3); **101** versus **99** (Table 4); **105** versus **104** (Table 5)). In the literature, analogues containing substituted β -amino acid units appended to various scaffolds have been widely studied as GPIIb-IIIa antagonists, and the β -amino acid unit has been postulated to mimic the β -carboxyl group of the aspartic acid residue of the RGD sequence.^{6e,7,11} Further lipophilic substitutions at both α - and β -positions of these units have generally enhanced potency and PK properties. However, in the 1-oxo- γ -spirocyclic lactam scaffold, a β -position methyl group (**53**, **81** versus **23** (Table 1)) did not improve potency. This may imply special conformational requirements for this rigid template.

Table 1. In Vitro Activity and Pharmacokinetic Parameters for the 1-Oxospirolactam Scaffold-Based Analogues: 4-(1-Oxo-2,8-diazaspiro[4.5]dec-2-yl)benzamidines

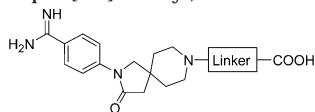
Compd. No.	-Linker-COOH	R	IC ₅₀ (μM) Binding ELISA ^b	IC ₅₀ (μM) PRP ^a	F%, rat (as ethyl ester prodrug)	t _{1/2β} (hr)	cLogP
77		H	15.8	12.5			1.73±0.77
78		H	5.6	0.733			1.9±0.75
28		H	0.004	0.054 (PPACK IC ₅₀ = 0.168) ^c	4.0	0.92	2.12±0.74
40b		Et	0.841	7.535			2.98±0.74
39b		Morpholine	4.185	5.50			1.64±0.8
79		H	6.0	3.4			2.4±0.73
72		H	7.80	5.183			1.77±0.69
44		H	0.004	0.112 (PPACK IC ₅₀ = 0.323) ^c			2.46±0.74
45		H	0.005	0.350			2.46±0.74
33		H	0.017	0.108 (PPACK IC ₅₀ = 0.260) ^c			2.11±0.83
48		H	0.090	0.149		0.50	3.79±0.75
69		H	0.005	0.066	2.27	0.86	3.87±0.81
59		H	0.005	0.036	not detected	2.4	2.14±1.11
63		H	0.001	0.066	not detected	0.71	2.05±0.94
23		H	0.004	0.053 (PPACK IC ₅₀ = 0.110) ^c	3.4	2.0	-0.25±0.77
53		H	0.005	0.068			0.30±0.69
81		H	0.004	0.122			0.30±0.69

^a Inhibition of platelet aggregation induced by 20 μM adenosine 5'-diphosphate (ADP) in citrated human platelet rich plasma (*h*-PRP).

^b Inhibition of the binding of fibrinogen to purified human GPIIb-IIIa in a 96-well format (ELISA assay). ^c Inhibition of platelet aggregation induced by 20 μM ADP in *h*-PRP with PPACK (see Experimental Section for details).

Hartman et al., Egbertson et al., and Xue et al.²² have reported that introduction of a sulfonamide or a carbamate substituent α to the carboxylate resulted in very potent and specific inhibitors of GPIIb-IIIa. These authors have suggested that this favorable effect is the result of an interaction with an exosite in the integrin. These α -substituents might also be functioning as a surrogate for the α -carboxylic acid of the Asp-residue.

This modification has been applied in our various series and was not found to be uniformly successful in enhancing the GPIIb-IIIa inhibitory activity of compounds. In the 1-oxo- γ -spirolactam series, α -sulfonamides (Table 1; **59**, **63**) or α -carbamate (**69**) substituents were close to equipotent with the parent compounds lacking substituents (**23**, **28**). The result is different from our observations in the hydantoin series (Table 3; **92**, **97**, **91**) and

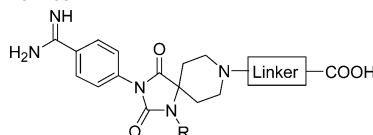
Table 2. In Vitro Activity and Pharmacokinetic Parameters for the 3-Oxospirolactam Scaffold-Based Analogues: 4-(3-Oxo-2,8-diazaspiro[4.5]dec-2-yl)benzamidines

Compd. No.	-Linker-COOH	IC ₅₀ (μM) Binding ELISA ^b	IC ₅₀ (μM) PRP ^a	F%, rat (as ethyl ester prodrug)	t _{1/2β} (hr)	cLogP
82		25.0	7.40			1.81±0.77
83		10.50	5.70			1.98±0.75
84		0.650	0.660			2.20±0.74
85		7.30	4.10			2.50±0.73
86		0.025	0.100	not detected	1.45	3.88±0.75
87		0.350	0.171	3.40	0.79	-0.17±0.77
75		15.0	3.60			1.16±0.77

^{a,b} See Table 1.

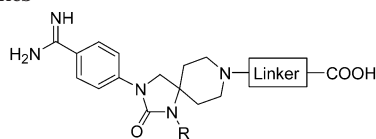
imide series (Table 5; **106**) in which such α -substitution leads to a significant improvement over the unsubstituted analogue in *h*PRP.

Numerous studies of GPIIb-IIIa inhibitors have suggested that residues at or very near the aspartic acid of the RGD sequence can also modulate the selectivity of ligand binding to integrins, and introduction of aromatic or other hydrophobic residues proximal to the RGD site can significantly enhance the inhibitory activity and specificity of the RGD analogues.²³ On the basis of an extensive SAR study at a position β -to the carboxylic acid terminus in a different series of GPIIb-IIIa inhibitors, Zablocki et al.²⁴ have reported the discovery of potent platelet aggregation inhibitor, xemilofiban (Figure 1). We have studied the effect of β -substitutions to the carboxylic acid in our spirocyclic series by incorporating methyl and phenyl substituents. In the 1-oxo- γ -spirolactam series, β -substituents were less active than the corresponding compounds lacking substituents (Table 1; **44**, **45**, **48**). Again, this result is opposite to what is observed in the hydantoin (**93**), urea (**103**), and 3-oxo- γ -spirolactam series (**86**). For these, β -substitution resulted in a

Table 3. In Vitro Activity and Pharmacokinetic Parameters for the Spirohydantoin Scaffold-Based Analogues: 4-(2,4-Dioxo-1,3,8-triazaspiro[4.5]dec-3-yl)benzamidines

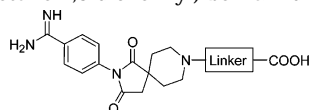
Compd. No.	-Linker-COOH	R	IC ₅₀ (μM) Binding ELISA ^b	IC ₅₀ (μM) PRP ^a	F% in rat (as ethyl ester prodrug)	t _{1/2β} (hr)	cLogP
89		Me	0.100	0.700			0.48±0.89
90		H	0.021	0.586			0.72±0.87
91		Me	0.020	0.065	only traces detected in rat plasma		2.23±0.95
92		Me	0.016	0.118			0.50±1.21
93		Me	0.032	0.120	<2.0	0.23	2.16±0.90
94		Me	0.050	0.222	2.42	0.85	-1.89±0.92
95		H	0.329	0.468			-1.65±0.90
96		Me	0.050	0.103	not detected	0.36	0.09±0.93
97		Me	0.002	0.059	not detected	1.73	0.41±1.07
98		Me	6.49	7.56			0.13±0.84

^{a,b} See Table 1.

Table 4. In Vitro Activity and Pharmacokinetic Parameters for the Spiroreurea Scaffold-Based Analogues: 4-(2-Oxo-1,3,8-triazaspiro[4.5]decan-2-one-3-yl)benzamidines

Compd. No.	-Linker-COOH	R	IC ₅₀ (μM) Binding ELISA ^b	IC ₅₀ (μM) PRP ^a	F% in rat (as ethyl ester prodrug)	cLogP
99		Me	1.02	0.674		1.70±0.75
100		H	0.751	1.018		0.65±0.74
101		Me	0.40	0.212	2%	-0.67±0.78
102		H	1.61	3.77		-1.71±0.78
103		Me	0.020	0.080	not detected	3.38±0.76

^{a,b} See Table 1.

Table 5. In Vitro Activity and Pharmacokinetic Parameters for the Spiroimide Scaffold-Based Analogues: 4-(1,3-Dioxo-2,8-diazaspiro[4.5]decan-1,3-dione-2-yl)-benzamidines

Compd. No.	-Linker-COOH	IC ₅₀ (μM) Binding ELISA ^b	IC ₅₀ (μM) PRP ^a	F%, rat (as ethyl ester prodrug)	t _{1/2 β} (hr)	cLogP
104		0.43	0.73			1.06±0.72
105		0.41	0.64			-1.31±0.75
106		0.030	0.27	4.3	0.9	2.81±0.79

^{a,b} See Table 1.

significant improvement over the unsubstituted analogue in *h*PRP (Tables 2–4).

Interestingly, all the templates investigated within the [4.5]-spirocyclic framework have provided potent compounds. This is consistent with the hypothesis that GPIIb-IIIa does not require significant interaction with the central template of inhibitors. Its sole purpose appears to be providing the scaffold to deliver the acidic and basic pharmacophores in the correct geometry to mimic the RGD sequence of fibrinogen receptor, which is believed to represent the minimal sequence necessary for binding to GPIIb-IIIa.

Of all the spirocyclic templates that we have investigated, the 1-oxo- γ -spiro lactam template has provided the most potent GPIIb-IIIa antagonists. Optimum binding to the RGD binding motif of the fibrinogen binding site in the basic framework was depicted in the compounds **28** and **23** (Table 1). Attempts to improve their activity by utilizing the SAR previously documented in the other GPIIb-IIIa antagonist templates proved fruitless. Interestingly, SAR in other spiro-scaffolds de-

scribed here has led to the expected enhancements in activity when modifications were made to the compounds.

Changing only the spirocyclic scaffold, a comparison of the inhibitory activities of compounds **23** (Table 1), **87** (Table 2), **94**, **95** (Table 3), **101**, **102** (Table 4), and **105** (Table 5) implies that the 1-oxo- γ -spiro lactam scaffold is in the appropriate rigid conformation to display the acidic and basic pharmacophores for optimum binding.

In Vivo Results. In general, GPIIb-IIIa antagonists containing both an amidine and a carboxylic acid group have very low oral bioavailability. This has been attributed both to the strongly basic nature of the amidine functionality and to the highly polar, acidic nature of the carboxylic acid. Analogues which display both groups are expected to behave as zwitterionic species. In particular, the strongly basic amidine group would be expected to exist in its ionic form both in the acidic conditions of the stomach and also in the weakly basic conditions of the intestine. This lasting ionic form could prevent the absorption through a passive transport from the intestine, which is greatly dependent on the lipophilicity of the molecule. In addition, the terminal carboxylic acid may also contribute to poor absorption. To circumvent these problems, various approaches have been aimed at both masking the basicity of the amidine group and enhancing the lipophilicity of the molecule.

When selected compounds from each spirocyclic scaffold were evaluated as their ethyl ester prodrugs in rat, they exhibited bioavailability of $\leq 5\%$, although some displayed encouraging elimination half-lives (Tables 1–5). Again, the strongly basic nature of the amidine group was considered a likely cause of the poor bioavailability.

In one approach aimed at finding a less basic substitute for the amidine group, GPIIb-IIIa antagonists where a pyridine or piperidine ring substitutes for the benzamidine have been explored (Figure 1, ZD-2486,²⁵ lotrafiban,²⁶ elarofiban,²⁷ UR-12947). However, when used in the spirocyclic scaffold series, the pyridine-

containing compounds did not show a favorable pharmacokinetic profile. This was despite retaining equivalent potency compared to the corresponding amidine analogues.¹⁵

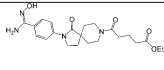
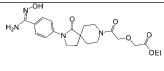
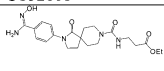
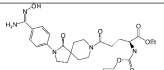
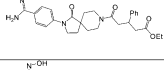
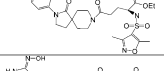
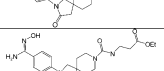
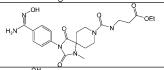
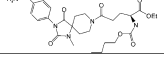
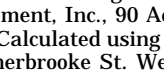
In another approach aimed at enhancing the lipophilicity of the overall molecule and also partially masking the charge on the amidine group, mono- and dialkylated amidino analogues have been investigated (Figure 1, NSL-96184, PSA0613). The dialkylated analogues have been found to retain their activity and exhibit improved PK profiles.²⁸ However, in the 1-oxo-spirolactam series, both mono- and disubstituted amidino analogues showed greatly diminished activity (Table 1; **40b** and **39b** versus **28**). This anomaly may also be rationalized by invoking the spatial-constraints of the centrally rigid spirocyclic template.

A double prodrug approach relies on the strategy of masking both polarizable pharmacophore groups in order to enhance oral bioavailability. Such an approach has been employed previously to obtain orally bioavailable GPIIb-IIIa antagonists, e.g. lefradafiban (BIBU-104) (methyl carbamate),²⁹ sibrafiban (Ro 48-3657) (amidoxime),³⁰ gantofiban³¹ (EMD-122347) (methyl carbamate) (Figure 1). In the novel amidoxime prodrug approach, aimed at lowering the pK_a of the basic benzamidine, the liver- and/or gut-mediated reduction of the amidoxime generates the active metabolite. Novel GPIIb-IIIa double prodrug containing antagonists with amidoxime and ethyl ester functionalities have been described which exhibit PK profiles in rats, dogs, and rhesus monkeys which are independent of the species. On the basis of these observations, we investigated this double prodrug strategy for our most potent spirocyclic compounds. The amidoxime ethyl ester double prodrugs described here were synthesized using the reaction sequence shown in Schemes 3 and 4. The pharmacokinetic data on the amidoxime ethyl ester double prodrugs, representing each spirocyclic scaffold, is depicted in Table 6. The double prodrugs of the spirourea and spirohydantoin-containing scaffolds (**111**, **112**, and **113**) did not show a noticeable improvement in bioavailability over their nonprotected version. However, for the 1-oxo-spirolactam series, a dramatic improvement was observed by the double prodrug approach. Three of the best of these (**22**, **27**, and **36**; Table 6) were chosen for further study.

The higher oral bioavailability observed for the 1-oxo-spirolactam series over other spirocyclic scaffolds may be attributed to its higher rigidity, optimal lipophilicity, and its lower polar surface area (Table 6). Reduced polar surface area has been suggested to correlate better with increased permeation rate than does lipophilicity ($cLogP$), and this should also help explain the difference in $F\%$ for the compounds within this lactam series which have similar $cLogP$ values (Table 1).³²

The differences in PK properties of compounds **22**, **110**, **111**, and **112** (Table 6) which differ only in the nature of the five-membered ring is noteworthy in this regard. Hydantoin- and urea-containing spiro templates have relatively more polar surface area and thus they would be expected to be less able to penetrate membranes. They indeed are less bioavailable. For the 1-oxo- and 3-oxospirolactams (**22** and **110**), one would expect the 3-oxo-carbonyl group in **110** to be more exposed to

Table 6. PK Properties of Active Drugs after Oral Administration of Double Prodrugs in Rats (1.0 mg/kg)

Prodrug/Drug	Prodrug	F% rat (po)	AUC ng*hr/ml	$cLogP^{a,c}$	3D PSA ^b (Å ²)	TPSA ^c (Å ²)
27/28	 CT51269	36.3	500.6	3.81±0.68	262.6	125.5
36/33	 CT52108	35.9	651	3.79±0.75	280.2	134.8
22/23	 CT51464	22.3	565.1	1.44±0.69	268.4	137.6
107/69	 CT51907	6.4	184	5.47±0.79	310.8	163.9
108/48	 CT51907	2.0	7.9	5.32±0.72	245.9	125.5
109/59	 CT51907	not detected		3.83±0.05	298.7	197.7
110/87	 CT51907	14.1	95.6	1.52±0.69	278.1	137.6
111/102	 CT51907	2.60	24.0	0.53±0.80	295.5	138.3
112/94	 CT51907	4.8	60.0	-0.69±0.93	300.7	155.4
113/91	 CT51907	not detected		3.92±0.88	346.2	184.2

^a Calculated using ACD/LogP version 4.56 (Advanced Chemistry Development, Inc., 90 Adelaide St. West, Toronto, Canada M5H 3V9). ^b Calculated using MOE (Chemical Computing Group, Inc., 1010 Sherbrooke St. West, #910, Montreal, Canada H3A 2R7). ^c Calculated using the method of Ertl.³⁴

Table 7. Pharmacokinetic Parameters of **23**, **28** and **33** after Oral Administration of **22**, **27**, and **36** in Rat (1.0 mg/kg)

compound	iv		po		F, %
	AUC, ng·h/mL	$t_{1/2\beta}$	AUC, ng·h/mL	$t_{1/2}$	
28 , CT50614	500.6	1.8	181.9	1.14	36.3
23 , CT50728	565.1	1.81	126.2	1.42	22.3
33 , CT51907	651	1.94	366.6	1.57	35.9

solvation than the corresponding 1-oxo-carbonyl group in **22**, as is reflected in their polar surface areas, and this may help explain the distinct differences in their PK profiles. This is noteworthy because for these two compounds all other physicochemical parameters are the same, including the number of rotatable bonds and the hydrogen-bond donor/acceptor groups.

The pharmacokinetic data, in rats, for the double prodrugs **22** (CT51464), **27** (CT51269), and **36** (CT52108) are shown in Table 7. This PK data indicates that all the double prodrugs are rapidly ($T_{max} = 1$ h) and well absorbed. All the drugs exhibited similar PK profiles. For example, after oral administration of **22**, at a dose of 1 mg/kg to male rats ($n = 6$) and the active drug (**23**) as well as amidoxime acid (**24**) were detected in plasma (Figure 2). While **23** showed a relatively long elimination half-life ($t_{1/2\beta} = 1.81$ h, mean), amidoxime **24** disappeared more rapidly ($t_{1/2\beta} = 0.6$ h \pm 0.03, mean \pm SD).

The double prodrug **22** was absorbed and converted to an active compound in vivo, most probably

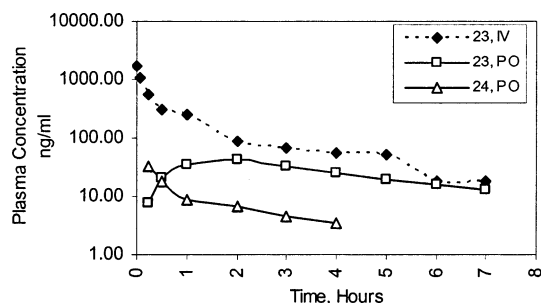


Figure 2. Plasma levels of **23** after iv administration of **23** (0.1 mg/kg) and po administration of **22** (1.0 mg/kg) versus time, as determined by LC/MS/MS in rats ($n = 6$). **24** is the corresponding amidoxime acid.

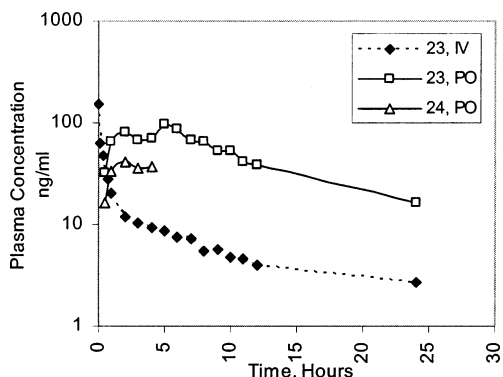


Figure 3. Plasma levels of **23** after iv administration of **23** (0.1 mg/kg) and po administration of **22** (1.0 mg/kg) versus time, as determined by LC/MS/MS in dogs ($n = 4$). **24** is the corresponding amidoxime acid.

to the amidino acid **24**. The metabolic reduction of benzamidoxime derivatives to benzamidines, in vivo as well as in vitro, is well documented.³³ The clearance mechanism for **24** has not been determined. Despite the two metabolic steps involved, the interindividual variability of the plasma concentration of active compound **23** was low. In either case, the rapid appearance of **24** suggests rapid absorption of prodrug. T_{max} for **24** after oral administration of **22** was 0.25 h, and that for **29** and **37** after oral administration of **27** and **36**, respectively, was ≤ 0.5 h. In a separate experiment, the amidoxime acid **29** exhibited low bioavailability in rats ($F = 3.7\%$).

The oral absorption of **22** (CT51464) may be a complicated process involving multiple absorption sites in the digestive tract. Metabolism of the double prodrug in the intestinal tract may also play a role in the absorption process. The rapid appearance of **24** and the delayed absorption maxima of **23** (Figure 2) may indicate a two-step absorption process. A portion of the drug may be absorbed from the stomach and/or proximal sections of the intestines while the remaining drug is absorbed in distal portions of the intestine. A second possibility for the delayed appearance of **23** may be that rapid absorption of the prodrug occurs but the intermediate product **24** or the active compound **23** forms a conjugate (glucuronic acid, sulfate, glycine, etc.) which is subsequently hydrolyzed to give **23**.

Figures 4, 5, and 6 show the PK profiles of **23**, **28**, and **33** in cynomolgus monkeys after iv administration of the active drugs **23**, **28**, and **33** and after oral administration of their respective double prodrugs (**22**, **27**, and **36**). From the in vivo data, the conversion of the ester

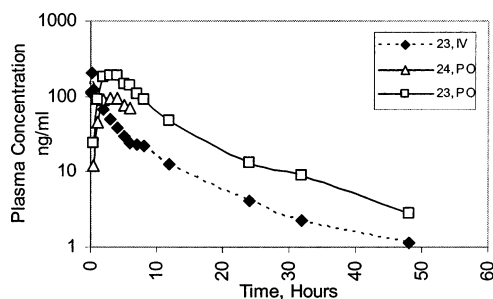


Figure 4. Plasma levels of **23** after iv administration of **23** (0.2 mg/kg) and po administration of **22** (2.0 mg/kg) versus time, as determined by LC/MS/MS in cynomolgus monkeys ($n = 4$). **24** is the corresponding amidoxime acid.

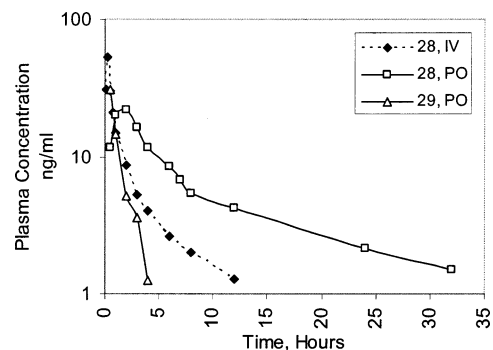


Figure 5. Plasma levels of **28** after iv administration of **28** (0.2 mg/kg) and po administration of **27** (2.0 mg/kg) versus time, as determined by LC/MS/MS in cynomolgus monkeys ($n = 4$). **29** is the corresponding amidoxime acid.

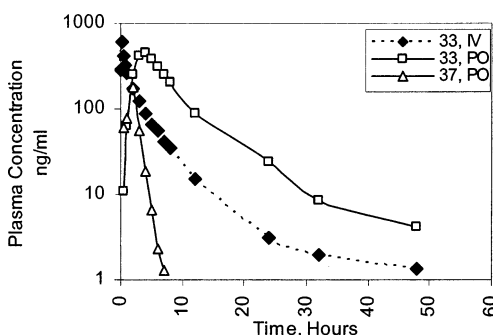


Figure 6. Plasma levels of **33** after iv administration of **33** (0.2 mg/kg) and po administration of **36** (2.0 mg/kg) versus time, as determined by LC/MS/MS in cynomolgus monkeys ($n = 4$). **37** is the corresponding amidoxime acid.

to the acid seems to be faster than the conversion of the N-hydroxyamidine to the amidine. The data may also suggest that the relative rates of absorption of the different structures may vary by species.

For **28/27** (Figure 5), pharmacokinetic patterns similar to those described above for rats were observed. The peak plasma level of amidoxime acid **29** was higher and was reached earlier ($T_{max} \leq 0.5$ h) than that of **28** ($T_{max} = 2$ h). For **33/36** (Figure 6), a similar PK profile was observed. However, for **23/22** (Figure 4), the peak plasma levels of amidoxime acid **24** were lower than that of **23**, even at 0.5 h when the first samples were drawn. T_{max} for **24** and **23** were the same (1.5–3.5 h).

The half-life of **28** in cynomolgus monkeys (8.9 h) is longer than that observed in rats (1.8 h). The affinity of **28** for the cynomolgus monkey GPIIb-IIIa receptor is stronger than that for rat ($IC_{50} = 0.128 \pm 0.031 \mu M$ versus $0.60 \pm 0.013 \mu M$), and we and others hypothesize

Table 8. Summary of Pharmacokinetic Parameters of **23**, **28**, and **33** after iv (1 mg/kg) and Oral Administration of **22**, **27**, and **36** in Rat, Dog, and Cyno

prodrug/drug	species	oral dose, mg/kg	<i>F</i> , % ^{a,c}		<i>t</i> _{1/2β} , h ^{a,b}		<i>V</i> _z , L/kg ^d		Cl, mL/min/kg	
			average	SD	average	SD	average	SD	average	SD
27/28	rat (6)	1	36.3	—	1.8	—	—	—	—	—
	dog (4)	1	39	16.3	10.3	3.5	5.75	1.04	6.44	1.16
	cyno (4)	2	18.77	1.2	8.9	2.4	5.02	5.26	6.51	6.83
22/23	rat (6)	1	22.3	—	1.81	—	—	—	—	—
	dog (4)	1	72.9	26.1	8.97	1.89	4.12	1.46	8.43	2.98
	cyno (4)	2	32.4	8.85	14.2	3.18	6.30	2.12	5.12	1.73
36/33	rat (6)	1	35.9	10	1.94	—	—	—	—	—
	dog (4)	1	23.3	3.9	10.3	1.35	2.93	0.32	3.28	0.36
	cyno (4)	2	30.6	3.41	7.51	2.16	1.75	0.22	2.70	0.34

^a Data are mean ± SD. ^b The apparent elimination half-life (*t*_{1/2β}) was determined from the linear portion of the log plasma concentration–time profile. ^c The bioavailability (*F*) of **23**, **28** and **33** after po administration of **22**, **27**, and **36** was calculated accounting for the differences in molecular weights and doses. ^d The volume of distribution (*V*_z) was calculated as dose/(AUCINF* λ_z) where λ_z is the terminal elimination rate constant. Lambda Z (λ_z) is calculated as the slope of the terminal, linear portion of the log linear plot of plasma concentration versus time.

Table 9. Activity Summary for Leading Candidates: Comparison to Sibrifiban and Orbofiban

	28 CT050614 (μM)	23 CT050728 (μM)	33 CT051907 (μM)	orbofiban (μM)	sibrifiban (μM)
Aggregation Assays (in PRP)					
20 μM ADP–citrate	0.054 (± 0.005)	0.053 (± 0.010)	0.108 (± 0.011)	0.068 (± 0.015)	0.051 (± 0.008)
20 μM ADP–PPACK	0.168 (± 0.010)	0.110 (± 0.019)	0.260 (± 0.029)	0.137 (± 0.038)	0.072 (± 0.017)
5 μM TRAP6–citrate	0.123 (± 0.021)	0.120 (± 0.047)	0.273 (± 0.080)	0.166* (± 0.008)	0.147* (± 0.017)
5 μM TRAP6–PPACK	0.368 (± 0.009)	0.365 (± 0.092)	0.691 (± 0.034)	0.362* (± 0.013)	0.182* (± 0.011)
4 μg/mL collagen–citrate	0.175 (± 0.009)	0.140 (± 0.045)	0.393 (± 0.049)	n.d.	n.d.
4 μg/mL collagen–PPACK	0.464 (± 0.073)	0.450 (± 0.072)	0.812 (± 0.187)	n.d.	n.d.
Solid-Phase Assays					
fibrinogen binding to GPIIb-IIIa	0.00367 (± 0.00104)	0.00390 (± 0.00128)	0.00976 (± 0.0021)	0.00238 (± 0.0032)	0.00114 (± 0.0002)
vitronectin binding to α _v β ₃	>50	>50	>50	n.d.	>50
Cell Adhesion Assays					
HUVEC adhesion to vitronectin	>50	>50	>50	n.d.	>50
HUVEC adhesion to fibronectin	>50	>50	>50	n.d.	>50

*211-47 TRAP was used for these determinations.

that the terminal half-life of the drug may be controlled to a large extent by its binding affinity to platelets.¹¹ Although this platelet binding hypothesis is in agreement with the half-life data obtained for **28**, no direct evidence exists to prove the hypothesis in this series.

When compound **22** was given orally to fasted male beagle dogs at 1 mg/kg (*n* = 4), a pharmacokinetic pattern similar to that described above for cynomolgus monkey was observed (Figure 3). The peak plasma levels of amidoxime acid **24** were lower than that of **23** even at 0.5 h. For both **23** and **24**, the *T*_{max} was about 5 h. The *t*_{1/2β} for **23** was 8.97 h. Compared to the experiment in monkeys, the half-life was longer and bioavailability was higher. The affinity of **23** for the dog GPIIb-IIIa receptor may be stronger than that for cyno (IC₅₀ = 0.239 ± 0.39 μM versus 0.410 ± 0.152 μM).

The pharmacokinetic data for **22**, **27**, and **36** is summarized in Table 8, and the comprehensive in vitro data in Table 9 along with data for orbofiban and sibrifiban. The three selected double prodrug analogues all exhibit good activity in human plasma, have low protein binding, and are stable in gastric juice, phosphate-buffered saline (PBS), and water. They also exhibit superior stability in human hepatic microsomes and do not inhibit the P450 3A4 isozyme (data not shown). All the final candidates were also found to

be negative in preliminary AMES tests. Virtually all the active compounds in this series demonstrated a selectivity of >5000-fold for GPIIb-IIIa versus the most closely related integrin, the vitronectin receptor α_vβ₃. **22** (CT51464) was eventually chosen for further development due to its superior bioavailability and half-life.

The relatively high oral bioavailability of **22** may obviate the problem of large plasma level variability from patient to patient, which has been postulated to be a drawback with previous oral GPIIb-IIIa antagonists that demonstrated no clear therapeutic benefits in Phase III clinical evaluation. The high bioavailability of **22** coupled with its long elimination half-life may also address the problem of a narrow therapeutic index leading to a narrow window of safety.

In Vivo Demonstration of GPIIb-IIIa Dependence of Mouse Bleeding Time. A platelet-dependent mouse tail bleeding time model was used to demonstrate the in vivo antithrombotic capacity of these potent GPIIb-IIIa antagonists. In this model, **59** (CT50787), a specific αIIBβ3 (GPIIb-IIIa) antagonist, was administered to prevent platelets from aggregating and forming the platelet plug necessary to promote hemostasis. GPIIb-IIIa antagonists are generally very species selective, and of the many spirocyclic analogues that were tested, **59** was determined to have the highest affinity

Table 10. Dose-Dependent Effect of **59** (CT50787) vs DMSO (Vehicle) on Bleeding Time in Mice

treatment regimen, mg/kg	<i>n</i>	mean BT (s)	SD	% of average vehicle control
vehicle control	15	116.0	30.4	
10	3	96.7	22.1	-17
40	4	196.5	81.4	69
50	4	562.5	161.4	385
100	8	890.6	26.5	668

for the mouse GPIIb-IIIa receptor with an *in vitro* IC₅₀ value of 48 nM.

To test the effects of **59** on mouse bleeding times, it was administered *iv* to female C57/bl mice in 10% DMSO in water at 10–100 mg/kg via a tail vein. Bleeding was initiated by transection of the tip of the tail, which was then immersed in a 37 °C normal saline bath. The bleeding time was recorded until cessation of blood flow by visual inspection or up to 15 min (900 s).

Because of the rapid clearance and a short half-life of **59** in rodents, maintaining an *in vivo* exposure level necessary to inhibit platelet aggregation and extend bleeding times was achieved by administering high doses via intravenous bolus injection. Table 10 shows the bleeding times in the presence and absence of **59**. A dose-dependent extension of bleeding time was demonstrated with *iv* administration of **59** with no effect at the lowest dose of 10 mg/kg and a near maximal effect, up to 668% of baseline, at the highest dose examined. *Ex vivo* aggregation measurements were not accomplished at the end of the bleeding time procedure due to the low level of drug in the plasma at the end of the 15 min time period.

Despite the limitation of not directly correlating the *in vivo* extension of bleeding time to *ex vivo* platelet aggregation inhibition, this experiment shows for the first time the use of a pharmacological agent which is α IIB β 3 specific to show extension of bleeding times in mice.³⁵ In addition, the dose dependent extensions of bleeding time shown in this study validates the platelet dependence of the mouse bleeding time model.

Conclusions

We have described the novel 2,8-diazaspiro[4.5]decane spirocyclic template for the disposition of pharmacophores to achieve potent and selective GPIIb-IIIa inhibition. Structural optimization within this scaffold has led to the characterization of a 1-oxo-spirolactam **23** (CT50728) as a novel, low molecular weight, selective, and reversible GPIIb-IIIa antagonist, with an IC₅₀ of 0.110 μ M for the inhibition of ADP-induced human platelet aggregation *in vitro*. While the parent active compound **23** has negligible oral bioavailability, its double prodrug **22** (CT51464) exhibits good oral bioavailability across species (rat, dog, monkey) and is rapidly metabolized to the active compound *in vivo*. We ascribe the excellent bioavailability of **22** to its molecular rigidity, low polar surface area, remarkably good water solubility as a crystalline hydrochloride salt (> 10 mg/mL), and its lipophilicity (log *P* = 0.45 \pm 0.06). Its p*K*_a values (p*K*_{a1} = 11.28, and p*K*_{a2} = 4.74) indicate that the drug remains uncharged over a wide range, and this could enhance oral absorption.

Other potent inhibitors in this series also exhibited the required PK profile, including bioavailability, long

elimination half-life, and metabolic stability. A favorable biological profile of these compounds as platelet aggregation inhibitors clearly demonstrates the utility of the spirocyclic structures as central templates for non-peptide RGD mimics. The easy synthesis of these templates and the useful oral pharmacokinetic profile of novel compounds containing these templates may facilitate their utilization in other drug targets.

Experimental Section

Unless otherwise noted, all starting materials were obtained from commercial suppliers and used without further purification. All reactions involving oxygen or moisture-sensitive compounds were performed under a dry argon atmosphere. All reaction mixtures and chromatography fractions were analyzed by thin-layer chromatography on 250 mm silica gel plates and visualized with UV light and I₂ stain. Flash column chromatography was carried out using Merck silica gel 60 (230–400 mesh). ¹H NMR spectra were recorded on a Varian Unity+400 instrument. Chemical shifts are expressed in ppm downfield from internal tetramethylsilane. Apparent multiplicities are designated as s, singlet; d, doublet; t, triplet; q, quartet; m, multiplet; b, broad. Low-resolution mass spectra were recorded with a HP 1100-MSD LC-MS spectrometer. High-resolution mass spectra (HRMS) were recorded with a Sciex Qstar time-of-flight high-resolution mass spectrometer coupled with an Agilent HPLC. All mass spectra were taken in the positive ion mode under electrospray ionization (ESI). Final compounds were purified by reverse-phase high-performance liquid chromatography (RP-HPLC) using a Waters 4000Prep, Waters 490E multiwavelength detector, and Vydac 218TP1022 column (10 μ m, C₁₈, 22 mm \times 250 mm). The new compounds synthesized were characterized by mass spectrometry (MS) and NMR, and purity was determined by HRMS and two RP-HPLC systems. We did not obtain melting points and elemental analyses of these compounds, as most of the derivatives were amorphous, hygroscopic, and prepared in small quantities. Purity of the compounds was confirmed by two diverse RP-HPLC systems using Waters 600 controller, Waters 996 photodiode array detector, and Keystone Beta Basic column (C₁₈, 4.6 mm \times 50 mm), analytical RP-HPLC run using 214 nm for detection. RP-HPLC (# 1): Gradient method utilized 5–85% CH₃CN/9 min in the H₂O mixture with 0.1% trifluoroacetic acid (TFA). RP-HPLC (# 2): Isocratic method using various % of CH₃CN for 20 min in the H₂O mixture with 0.1% trifluoroacetic acid (TFA) in order to have the compound elute at a reasonable time during the run.

The typical experimental procedures, used in this study, for the conversion of benzonitriles to benzamidines are described below.

Typical Procedure A. Benzamidines from Benzonitriles via Thio-Pinner Synthesis.^{16a} (a) H₂S gas was bubbled into a solution of the benzonitrile (1.0 mmol) in 5.0 mL of the solvent mixture pyridine/Et₃N (9:1) until a deep green color persisted. The reaction mixture was then stirred overnight at room temperature, concentrated, and partitioned between 5% MeOH/CH₂Cl₂ and H₂O (3 \times). The combined organic extract was washed with brine, dried over Na₂SO₄, and concentrated to yield the thioamide as a yellow/green solid. (b) The thioamide was then dissolved in acetone (2.50 mL) and treated with CH₃I (5.0 mmol). The clear solution was stirred overnight at room temperature, and the resulting yellow suspension was concentrated to dryness to yield thiomethylimidate as a bright yellow solid. (c) The thiomethylimidate was mixed with NH₄OAc (25.0 mmol), MeOH (5.0 mL) was added, and the reaction mixture was either stirred overnight at room temperature or refluxed for 2.0 h. After TLC/RP-HPLC showed the complete consumption of the thiomethylimidate, methanol was removed by rotary evaporation, and the benzamidine was purified by prep RP-HPLC as either TFA or HCl salt.

Typical Procedure B. Synthesis of the N-Substituted Benzamidines (39a, 40a) from Benzonitriles via Thio-Pinner Route. For the synthesis of the N-substituted ben-

amidines (**39a** and **40a**), in step c of "Typical Procedure A," appropriate amine (EtNH₂, morpholine) was first treated with AcOH (2.0 equiv) in MeOH, and then this mixture was added to the thiomethylimidate. The resulting reaction mixture was stirred at room temperature, concentrated, and purified by prep RP-HPLC to afford the N-substituted-benzamidines.

Typical Procedure C. Benzamidines from Benzonitriles via Benzamidoximes.^{16b} (a) To benzonitrile (10.0 mmol) in EtOH (50.0 mL) was added Et₃N (50.0 mmol), followed by hydroxylamine hydrochloride (30.0 mmol), and the reaction mixture was either stirred overnight at room temperature or heated to 60 °C for 5.0 h until RP-HPLC indicated complete consumption of the benzonitrile. Then the reaction mixture was concentrated under reduced pressure and purified by prep RP-HPLC to afford pure benzamidoximes. (b) The benzamidoxime (5.0 mmol) was dissolved in glacial acetic acid (25.0 mL), and acetic anhydride (7.50 mmol) was added. After 0.5 h, RP-HPLC indicated complete consumption of the starting material. Then to it was added 10% Pd/C (15 wt %), and the mixture was shaken on a Parr hydrogenator at 40 psi H₂ for 5.0 h until RP-HPLC indicated no unreacted starting material. The reaction mixture was filtered through Celite and concentrated under reduced pressure to yield crude benzamidine, which was purified by prep RP-HPLC.

1-Benzyl-4-cyanomethylpiperidine-4-carbonitrile (1). To a stirred solution of 1-benzyl-4-piperidone (50.0 g, 264.20 mmol) and ethyl cyanoacetate (39.0 g, 344.80 mmol) in CH₂Cl₂ (300 mL) was added Et₃N (75.0 mL, 538.10 mmol) dropwise. Then crushed 4 Å molecular sieves (25 g) were added, and the mixture was stirred at room temperature until TLC check showed complete consumption of 1-benzyl-4-piperidone. The reaction mixture was filtered through Celite, and the filtrate was concentrated to yield (1-benzylpiperidin-4-ylidene)cianoacetic acid ethyl ester as a light yellow syrup.

This was then dissolved in EtOH (500 mL) and treated with a solution of KCN (85.0 g, 1.30 mol) in H₂O (200 mL). The brown solution was heated to reflux for 2.0 h, then concentrated to half its volume, and extracted with EtOAc (3 ×). The combined EtOAc extract was washed with brine, dried over Na₂SO₄, and concentrated to yield a brown solid. Flash chromatography using EtOAc/hexane furnished pure **1**, 55.10 g (87%). ¹H NMR (DMSO-*d*₆): δ 7.26 (m, 5H), 3.43 (s, 2H), 3.04 (s, 2H), 2.80 (d, 2H), 2.04 (m, 2H), 1.86 (d, 2H), 1.61 (m, 2H). MS (ES): 240 (M + H)⁺.

1-Benzyl-4-carboxymethylpiperidine-4-carboxylic Acid Hydrochloride (2). A suspension of dinitrile **1** (50.0 g, 208.92 mmol) in concentrated HCl (750 mL) was refluxed for 3 days. Then the pale yellow solution was concentrated to dryness to afford the diacid **2** as an off-white solid, as its hydrochloride salt, 64.0 g (98%). ¹H NMR (DMSO-*d*₆): δ 11.0 (m, 2H), 7.60 (s, 2H), 7.45 (s, 3H), 4.24 (dd, 2H), 3.11 (d, 1H), 3.05 (s, 2H), 2.90 (q, 1H), 2.40 (s, 2H), 2.08 (d, 2H), 1.88 (t, 2H). MS (ES): 278 (M + H)⁺.

4-(8-Benzyl-1,3-dioxo-2,8-diazaspiro[4.5]dec-2-yl)benzonitrile (4). To a stirred solution of the diacid hydrochloride (**2**) (4.70 g, 15.0 mmol) in DMF (50 mL) was added DCC (4.10 g, 19.87 mmol), and the slurry was stirred at room temperature for 2.0 h to furnish the anhydride (**3**). To it was added 4-aminobenzonitrile (2.20 g, 18.62 mmol) and Et₃N (6.0 mL, 43.0 mmol). The suspension was stirred overnight at room temperature, filtered through Celite, and concentrated to yield 1-benzyl-4-[(4-cyano-phenylcarbamoyl)-methyl]-piperidine-4-carboxylic acid as a pale yellow syrup. This was then suspended in acetic anhydride (75 mL), mixed with anhyd NaOAc (4.50 g, 54.85 mmol), and refluxed for 2.0 h. The reaction mixture was filtered through Celite, concentrated to dryness, and partitioned between 5% MeOH-CH₂Cl₂/H₂O (3 ×). The organic extract was washed with brine, dried over Na₂SO₄, and concentrated. Flash chromatography using CH₂Cl₂/MeOH afforded pure **4**, as a colorless solid, 3.40 g (63%). ¹H NMR (DMSO-*d*₆): δ 7.93 (d, 2H), 7.5 (d, 2H), 7.3 (m, 4H), 7.2 (m, 1H), 3.43 (s, 2H), 2.73 (m, 4H), 2.01 (t, 2H), 1.85 (t, 2H), 1.72 (d, 2H). MS (ES): 360 (M + H)⁺.

4-(8-Benzyl-1-oxo-2,8-diazaspiro[4.5]dec-2-yl)benzonitrile (7) and 4-(8-Benzyl-3-oxo-2,8-diazaspiro[4.5]dec-2-yl)benzonitrile (8). To a suspension of imide **4** (500 mg, 1.39 mmol) in MeOH (30 mL) at 0 °C was added NaBH₄ (275 mg, 7.27 mmol) in lots, and the mixture was stirred at room temperature until TLC showed complete consumption of the starting material. Then the reaction was quenched with AcOH and concentrated to dryness to yield a mixture of **5** and **6** (1:2 by NMR, and analytical RP-HPLC).

The whole was then dissolved in TFA (25 mL) at 0 °C and treated with NaBH₄ (250 mg, 6.61 mmol) in lots (*caution: reaction is extremely vigorous!*). The reaction mixture was stirred at room temperature until TLC showed no starting material, concentrated to dryness, and partitioned between CH₂Cl₂/1 N NaOH (3 ×). The CH₂Cl₂ extract was washed with brine, dried over Na₂SO₄, and concentrated to yield a colorless solid. Purification by RP-HPLC yielded **7** (97 mg) and **8** (210 mg), in 64% overall yield.

4-(8-Benzyl-3-oxo-2,8-diazaspiro[4.5]dec-2-yl)benzonitrile (8). ¹H NMR (CDCl₃): δ 7.78 (d, 2H), 7.62 (d, 2H), 7.3 (m, 5H), 3.62 (s, 2H), 3.56 (s, 2H), 2.56 (m, 4H), 2.40 (m, 4H), 1.71 (m, 4H). MS (ES): 346 (M + H)⁺.

2-(4-Cyanophenyl)-1-oxo-2,8-diazaspiro[4.5]decane-8-carboxylic Acid 2,2,2-Trichloroethyl Ester (9), and 2-(4-Cyanophenyl)-3-oxo-2,8-diazaspiro[4.5]decane-8-carboxylic Acid 2,2,2-trichloroethyl Ester (10). The mixture of lactams **7** and **8** (2.30 g, 6.66 mmol) in CH₃CN/CH₂Cl₂ (8:2) (40 mL) was treated with 2,2,2-trichloroethyl chloroformate (1.20 mL, 8.71 mmol), and the reaction mixture was stirred overnight at room temperature. Then all the solvents were evaporated, and the crude product was purified by flash chromatography (5% CH₃CN/CH₂Cl₂) to afford **9** (792 mg) and **10** (1.633 g); combined yield 85%.

2-(4-Cyanophenyl)-1-oxo-2,8-diazaspiro[4.5]decane-8-carboxylic Acid 2,2,2-trichloroethyl Ester (9). ¹H NMR (CDCl₃): δ 7.79 (d, 2H), 7.61 (d, 2H), 4.73 (q, 2H), 4.05 (m, 2H), 3.81 (t, 2H), 3.30 (m, 2H), 2.12 (m, 2H), 1.96 (m, 2H), 1.56 (m, 2H). MS (ES): 430 (M + H)⁺.

2-(4-Cyanophenyl)-3-oxo-2,8-diazaspiro[4.5]decane-8-carboxylic Acid 2,2,2-trichloroethyl Ester (10). ¹H NMR (CDCl₃): δ 7.72 (d, 2H), 7.62 (d, 2H), 4.73 (q, 2H), 3.78 (m, 2H), 3.67 (s, 2H), 3.4 (m, 2H), 2.6 (s, 2H), 1.75 (m, 4H). MS (ES): 430 (M + H)⁺.

4-(1-Oxo-2,8-diazaspiro[4.5]dec-2-yl)benzonitrile (11). To a solution of TCE-carbamate **9** (740 mg, 1.718 mmol) in THF (10 mL), under argon, was added 10 mL of a 1 M solution of NH₄OAc in H₂O (10 mmol), followed by 10% Cd-Pb couple¹⁸ (1.20 g, 9.0 mmol of Cd). The cloudy suspension was stirred at room temperature until TLC showed disappearance of starting material. Then the reaction mixture was filtered through Celite, the aqueous layer was made basic with 1 N NaOH, and extracted with CH₂Cl₂ (3 ×). The combined CH₂Cl₂ extract was washed with brine, dried over Na₂SO₄, concentrated, and chromatographed to yield **11**, 325 mg (74%). ¹H NMR (CDCl₃): δ 7.8 (d, 2H), 7.63 (d, 2H), 3.78 (m, 2H), 3.1 (m, 2H), 2.72 (t, 2H), 2.13 (t, 2H), 1.88 (m, 2H), 1.48 (m, 2H). MS (ES): 256 (M + H)⁺.

4-(3-Oxo-2,8-diazaspiro[4.5]dec-2-yl)benzonitrile (12). This compound was prepared from TCE-carbamate **10** using the method described above for the synthesis of **11**. Colorless solid, yield 89%. ¹H NMR (DMSO-*d*₆): δ 7.8 (q, 4H), 3.62 (s, 2H), 2.65 (m, 4H), 2.42 (s, 2H), 1.43 (m, 4H). MS (ES): 256 (M + H)⁺.

1-Benzyl-4-methylaminopiperidine-4-carbonitrile (13b). To a mixture of 1-benzyl-4-piperidone (47.32 g, 0.25 mol) and methylamine hydrochloride (16.90 g, 0.25 mol) in 1:1 MeOH/H₂O (100 mL), under stirring and at 0 °C, was added a solution of KCN (16.30 g, 0.25 mol) in H₂O (40 mL) dropwise, and the mixture was stirred overnight at room temperature. It was then diluted with Et₂O/H₂O (150 mL/75 mL) and transferred to a separatory funnel. The aqueous layer was extracted with ether (2 ×), and the combined ether extract was washed with brine, dried over Na₂SO₄, and concentrated to yield **13b**, 53.90 g (94%). ¹H NMR (CDCl₃): δ 7.29 (m, 5H), 3.53 (s, 2H), 2.80

(d, 2H), 2.50 (s, 3H), 2.34 (d, 2H), 2.0 (d, 2H), 1.71 (m, 2H). MS (ES): 230 (M + H)⁺.

1-(1-Benzyl-4-cyanopiperidin-4-yl)-3-(4-cyanophenyl)-1-methylurea (14b). To a solution of 4-cyanophenyl isocyanate (10.60 g, 73.54 mmol) in CH₂Cl₂ (75 mL) at 0 °C was added a solution of **13b** (17.0 g, 74.13 mmol) in CH₂Cl₂ (35 mL), followed by Et₃N (14.0 mL, 100.44 mmol). After stirring overnight at room temperature, the reaction mixture was concentrated to dryness and recrystallized from CH₂Cl₂/MeOH/hexane (150/10/100 mL) to afford **14b** as a colorless solid, 25.20 g (92%). ¹H NMR (CDCl₃): δ 7.5 (t, 2H), 7.28 (m, 4H), 7.11 (m, 1H), 3.62 (s, 2H), 2.96 (m, 5H), 2.78 (m, 2H), 2.09 (m, 2H), 1.90 (d, 2H). MS (ES): 374 (M + H)⁺.

1-(1-Benzyl-4-cyanopiperidin-4-yl)-3-(4-cyanophenyl)-urea (14a). This compound was prepared starting from 1-benzyl-4-piperidone using the procedures described above for **14b** and substituting methylamine hydrochloride with NH₄-Cl in the first step (Scheme 2), in an overall yield of 74%, as a colorless solid. ¹H NMR (DMSO-*d*₆): δ 9.25 (s, 1H), 8.81 (s, 1H), 7.86 (d, 2H), 7.70 (d, 2H), 7.2–7.35 (m, 5H), 3.49 (s, 2H), 2.72 (m, 2H), 2.30 (m, 2H), 2.01 (m, 2H), 1.52 (d, 2H). MS (ES): 360 (M + H)⁺.

4-(8-Benzyl-1-methyl-2,4-dioxo-1,3,8-triazaspiro[4.5]dec-3-yl)benzotrile (15b). **14b** (3.0 g, 8.033 mmol) was suspended in 1 N HCl (100 mL) and refluxed for 16 h. The clear reaction mixture was then concentrated to dryness, suspended in CH₂Cl₂, washed with 1 N NaOH and brine, dried over Na₂SO₄, and concentrated. The crude product was triturated with ether to afford **15b** as a colorless solid, 2.68 g (89%). ¹H NMR (CDCl₃): δ 7.74 (d, 2H), 7.64 (d, 2H), 7.28 (m, 5H), 3.62 (s, 2H), 2.96 (s, 3H), 2.82 (m, 4H), 2.14 (m, 2H), 1.76 (m, 2H). MS (ES): 375 (M + H)⁺.

4-(8-Benzyl-2,4-dioxo-1,3,8-triazaspiro[4.5]dec-3-yl)-benzotrile (15a). This compound was prepared from **14a** using the method described above for **15b**, as a colorless solid (80%). ¹H NMR (DMSO-*d*₆): δ 9.14 (s, 1H), 7.91 (d, 2H), 7.62 (d, 2H), 7.28 (m, 4H), 7.22 (m, 1H), 3.48 (s, 2H), 2.71 (m, 2H), 2.13 (m, 2H), 1.92 (m, 2H), 1.71 (m, 2H). MS (ES): 361 (M + H)⁺.

4-(1-Methyl-2,4-dioxo-1,3,8-triazaspiro[4.5]dec-3-yl)-benzotrile (19b). This compound was synthesized from **15b**, using the procedure described above for the preparation of **11** from **7**. (a) To **15b** (1.70 g, 4.54 mmol) in CH₃CN/CHCl₃ (20/10 mL) at room temperature was added 2,2,2-trichloroethyl chloroformate (1.0 mL, 7.264 mmol), and the mixture was stirred at room temperature for 6 h. Then it was concentrated to dryness and purified by flash chromatography to afford the TCE-carbamate intermediate, 3-(4-cyanophenyl)-1-methyl-2,4-dioxo-1,3,8-triazaspiro[4.5]decane-8-carboxylic acid 2,2,2-trichloroethyl ester, 1.80 g (86%). (b) To a stirred solution of the TCE-carbamate (1.80 g, 3.91 mmol) in THF (20 mL), under argon, was added 20 mL of a 1 M solution of NH₄OAc in H₂O (20 mmol), followed by 10% Cd–Pb couple (2.70 g, 20.2 mmol of Cd). The suspension was stirred overnight at room temperature and then filtered through Celite, and the aqueous layer was made basic with 1 N NaOH and extracted with CH₂Cl₂ (3 ×). The CH₂Cl₂ extract was washed with brine, dried over Na₂SO₄, concentrated, and chromatographed to yield **19b**, as a colorless solid, 880 mg (79%). ¹H NMR (CD₃OD): δ 7.80 (d, 2H), 7.63 (d, 2H), 3.27 (m, 2H), 2.99 (m, 2H), 2.91 (s, 3H), 1.97 (m, 2H), 1.80 (m, 2H). MS (ES): 285 (M + H)⁺.

4-(8-Benzyl-1-methyl-2-oxo-1,3,8-triazaspiro[4.5]dec-3-yl)benzotrile (17b). The urea **17b** was synthesized from the hydantoin **15b** using the previously described procedure for the synthesis of **7** and **8** from **4**. (a) To a suspension of the hydantoin **15b** (800 mg, 2.136 mmol) in MeOH (30 mL) at 0 °C was added NaBH₄ (400 mg, 10.57 mmol) in lots, and the mixture was stirred overnight at room temperature. Then the reaction was quenched with AcOH (1.0 mL) at 0 °C, and concentrated to dryness to afford crude 4-(8-benzyl-4-hydroxy-1-methyl-2-oxo-1,3,8-triazaspiro[4.5]dec-3-yl)benzotrile **16b**. (b) The crude **16b** was then dissolved in TFA (35 mL) at 0 °C and treated with NaBH₄ (400 mg, 10.57 mmol) in lots (*caution: reaction is extremely vigorous*). The reaction mixture was

stirred overnight at room temperature and then concentrated to dryness and partitioned between CH₂Cl₂/1 N NaOH (3 ×). The CH₂Cl₂ extract was washed with brine, dried over Na₂SO₄, and concentrated to yield a colorless solid, which was purified by RP-HPLC to yield **17b** as a colorless solid, 562 mg (73%). ¹H NMR (CDCl₃): δ 7.65 (d, 2H), 7.55 (d, 2H), 7.28 (m, 5H), 3.60 (s, 2H), 3.55 (s, 2H), 2.96 (m, 2H), 2.79 (s, 3H), 2.08 (m, 4H), 1.48 (m, 2H). MS (ES): 361 (M + H)⁺.

3-([2-(4-Cyanophenyl)-1-oxo-2,8-diazaspiro[4.5]decane-8-carbonyl]amino)propionic Acid Ethyl Ester (20). To a stirred solution of **11** (500 mg, 1.958 mmol) in CH₂Cl₂ (25 mL) at 0 °C was added ethyl-3-isocyanatopropionate (300 mg, 2.10 mmol), followed by Et₃N (320 μL, 2.30 mmol), and the mixture was stirred at room temperature for 9 h. The reaction was then quenched with H₂O (200 μL), concentrated to dryness, and purified by flash chromatography (5% MeOH/CH₂Cl₂) to afford **20**, 715 mg (92%). ¹H NMR (CDCl₃): δ 7.75 (d, 2H), 7.60 (d, 2H), 5.30 (m, 1H), 4.02 (q, 2H), 3.81 (t, 2H), 3.46 (m, 2H), 3.38 (m, 2H), 3.06 (m, 2H), 2.48 (m, 2H), 2.10 (t, 2H), 1.90 (m, 2H), 1.51 (m, 2H), 1.22 (t, 3H). MS (ES): 399 (M + H)⁺.

3-([2-(4-Carbamimidoylphenyl)-1-oxo-2,8-diazaspiro[4.5]decane-8-carbonyl]amino)propionic Acid Ethyl Ester (21). Compound **21** was synthesized from **20** using Typical Procedure A. (a) H₂S gas was bubbled into a solution of **20** (125 mg, 0.313 mmol) in 5.0 mL of pyridine/Et₃N (9:1) until a deep green color persisted. After stirring overnight at room temperature, the mixture was concentrated and partitioned between 5% MeOH/CH₂Cl₂ and H₂O (3 ×). The organic extract was washed with brine, dried over Na₂SO₄, and concentrated to yield 3-([1-oxo-2-(4-thiocarbamoylphenyl)-2,8-diazaspiro[4.5]decane-8-carbonyl]amino)propionic acid ethyl ester as a yellow/green solid. (b) This was then dissolved in acetone (5.0 mL), CH₃I (195 μL, 3.13 mmol) was added, and the reaction mixture was stirred overnight at room temperature. The yellow suspension was concentrated to dryness to afford 3-([2-(4-methylsulfanylcarbonimidoylphenyl)-1-oxo-2,8-diazaspiro[4.5]decane-8-carbonyl]amino)propionic acid ethyl ester as a yellow solid. (c) This was then dissolved in MeOH (5.0 mL) and NH₄OAc (600 mg, 7.78 mmol) was added. The reaction mixture was stirred overnight at room temperature, concentrated to dryness, and purified by RP-HPLC to afford **21** as its HCl salt, as a colorless solid, 98 mg (75% overall from **20**). ¹H NMR (CD₃OD): δ 9.11 (s, 1H), 8.68 (s, 2H), 7.98 (d, 2H), 7.83 (d, 2H), 4.13 (q, 2H), 3.94 (m, 2H), 3.45 (t, 2H), 3.11 (m, 2H), 2.54 (m, 2H), 2.22 (t, 2H), 1.83 (m, 2H), 1.61 (m, 2H), 1.24 (t, 3H). MS (ES): 416 (M + H)⁺. Exact mass (FAB, M + 1)⁺ calcd, 416.2220; found, 416.2239.

3-([2-(4-Carbamimidoylphenyl)-1-oxo-2,8-diazaspiro[4.5]decane-8-carbonyl]amino)propionic Acid (23) (CT50728). **21** (40 mg, 0.096 mmol) in THF (5.0 mL) was treated with 1 M LiOH (1.0 mL), and the reaction mixture was stirred at room temperature for 6 h. Then it was cooled in ice, acidified with 6 N HCl, concentrated to dryness, and purified by RP-HPLC to afford **23** as a colorless solid as its TFA salt, 43 mg (89%). ¹H NMR (CD₃OD): δ 7.92 (d, 2H), 7.79 (d, 2H), 3.87 (m, 3H), 3.38 (t, 2H), 3.30 (m, 1H), 3.05 (t, 2H), 2.47 (m, 2H), 2.18 (t, 2H), 1.80 (m, 2H), 1.55 (d, 2H). MS (ES): 388 (M + H)⁺. Exact mass (FAB, M + 1)⁺ calcd, 388.1979; found, 388.1944.

3-([2-[4-(N-Hydroxycarbamimidoyl)phenyl]-1-oxo-2,8-diazaspiro[4.5]decane-8-carbonyl]amino)propionic Acid Ethyl Ester (22) (CT51464). To **20** (1.13 g, 2.836 mmol) in EtOH (25 mL) was added Et₃N (1.60 mL, 11.48 mmol), followed by hydroxylamine hydrochloride (590 mg, 8.49 mmol). The reaction mixture was then stirred overnight at room temperature, concentrated, and purified by RP-HPLC to afford **22** as its HCl salt, 1.052 g (79%). ¹H NMR (CD₃OD): δ 7.93 (d, 2H), 7.70 (d, 2H), 4.12 (q, 2H), 3.91 (m, 4H), 3.40 (m, 2H), 3.06 (m, 2H), 2.51 (m, 2H), 2.20 (m, 2H), 1.81 (m, 2H), 1.56 (m, 2H), 1.23 (t, 3H). MS (ES): 432 (M + H)⁺. Exact mass (FAB, M + 1)⁺ calcd, 432.2241; found, 432.2254.

3-([2-[4-(N-Hydroxycarbamimidoyl)phenyl]-1-oxo-2,8-diazaspiro[4.5]decane-8-carbonyl]amino)propionic Acid (24). The ethyl ester **22** (215 mg, 0.498 mmol) was treated with

3 N HCl (5.0 mL) and the mixture was stirred at room temperature for 8 h. It was then concentrated, and purified by RP-HPLC to afford **24** as its HCl salt, 203 mg (92%). ¹H NMR (CD₃OD): δ 7.88 (d, 2H), 7.67 (d, 2H), 3.88 (t, 4H), 3.38 (t, 2H), 3.05 (t, 2H), 2.48 (t, 2H), 2.18 (t, 2H), 1.80 (t, 2H), 1.53 (d, 2H). MS (ES): 404 (M + H)⁺. Exact mass (FAB, M + 1)⁺ calcd, 404.1928; found, 404.1889.

5-[2-(4-Cyanophenyl)-1-oxo-2,8-diazaspiro[4.5]dec-8-yl]-5-oxopentanoic Acid Ethyl Ester (25). To **11** (150 mg, 0.587 mmol) in DMF (3.0 mL) at 0 °C was added DIEA (180 μL, 1.03 mmol), followed by ethyl glutaryl chloride (136 mg, 0.761 mmol), and the reaction mixture was stirred at room temperature for 4 h. Then it was partitioned between CH₂-Cl₂/satd NaHCO₃. The combined CH₂Cl₂ extract was washed with brine, dried over Na₂SO₄, concentrated, and purified by flash chromatography to afford **25**, 214 mg (92%). ¹H NMR (CDCl₃): δ 7.78 (d, 2H), 7.62 (d, 2H), 4.25 (m, 1H), 4.07 (q, 2H), 3.87 (m, 1H), 3.80 (m, 2H), 3.25 (m, 1H), 3.12 (m, 1H), 2.36 (m, 4H), 2.10 (m, 2H), 1.92 (m, 4H), 1.54 (m, 2H), 1.21 (t, 3H). MS (ES): 398 (M + H)⁺.

5-[2-(4-Carbamimidoylphenyl)-1-oxo-2,8-diazaspiro[4.5]dec-8-yl]-5-oxopentanoic Acid Ethyl Ester (26). Compound **25** was converted to **26**, using Typical Procedure A, elaborated above for the synthesis of **21** from **20**. Overall yield, 68%. ¹H NMR (CD₃OD): δ 7.92 (d, 2H), 7.80 (d, 2H), 4.28 (m, 1H), 4.07 (q, 2H), 3.93 (m, 3H), 3.32 (m, 1H), 3.05 (m, 1H), 2.44 (t, 2H), 2.35 (t, 2H), 2.21 (m, 2H), 1.85 (m, 2H), 1.76 (m, 2H), 1.61 (m, 2H), 1.20 (t, 3H). MS (ES): 415 (M + H)⁺. Exact mass (FAB, M + 1)⁺ calcd, 415.2339; found, 415.2313.

5-[2-(4-Carbamimidoylphenyl)-1-oxo-2,8-diazaspiro[4.5]dec-8-yl]-5-oxopentanoic Acid (28) (CT50614). The ethyl ester **26** (57 mg, 0.137 mmol) was suspended in 3 N HCl (2.0 mL) and the reaction mixture was stirred overnight at room temperature. Then it was concentrated, and purified by RP-HPLC to afford **28**, 49 mg (92%). ¹H NMR (CD₃OD): δ 7.80 (d, 2H), 7.68 (d, 2H), 4.17 (m, 1H), 3.8 (m, 3H), 3.21 (m, 1H), 2.94 (m, 1H), 2.33 (t, 2H), 2.23 (t, 2H), 2.10 (m, 2H), 1.6–1.8 (m, 4H), 1.52 (m, 2H). MS (ES): 387 (M + H)⁺. Exact mass (FAB, M + 1)⁺ calcd, 387.2026; found, 387.2017.

5-[2-[4-(N-Hydroxycarbamimidoyl)phenyl]-1-oxo-2,8-diazaspiro[4.5]dec-8-yl]-5-oxopentanoic Acid Ethyl Ester (27) (CT51269). To **25** (400 mg, 1.006 mmol) in EtOH (10 mL) was added Et₃N (420 μL, 3.01 mmol), followed by hydroxylamine hydrochloride (174 mg, 2.50 mmol). The mixture was stirred overnight at room temperature, concentrated, and purified by RP-HPLC to afford **27** as its HCl salt, as a colorless solid, 390 mg (83%). ¹H NMR (CD₃OD): δ 7.85 (d, 2H), 7.66 (d, 2H), 4.35 (m, 1H), 4.05 (q, 2H), 3.80 (m, 3H), 3.31 (t, 1H), 3.04 (t, 1H), 2.43 (t, 2H), 2.34 (m, 2H), 2.18 (t, 2H), 1.83 (m, 2H), 1.74 (m, 2H), 1.60 (m, 2H), 1.17 (t, 3H). MS (ES): 431 (M + H)⁺. Exact mass (FAB, M + 1)⁺ calcd, 431.2288; found, 431.2294.

5-[2-[4-(N-Hydroxycarbamimidoyl)phenyl]-1-oxo-2,8-diazaspiro[4.5]dec-8-yl]-5-oxopentanoic Acid (29). The ethyl ester **27** (160 mg, 0.37 mmol) was treated with 3 N HCl (2.0 mL), and the reaction mixture was stirred at room temperature for 9 h. Then it was concentrated, and purified by RP-HPLC to afford **29** as its HCl salt, 155 mg (95%). ¹H NMR (CD₃OD): δ 7.87 (d, 2H), 7.64 (d, 2H), 4.25 (m, 1H), 3.90 (m, 3H), 3.29 (m, 1H), 3.01 (m, 1H), 2.40 (t, 2H), 2.30 (t, 2H), 2.17 (m, 2H), 1.81 (m, 2H), 1.72 (m, 2H), 1.57 (m, 2H). MS (ES): 403 (M + H)⁺. Exact mass (FAB, M + 1)⁺ calcd, 403.1975; found, 403.2002.

tert-Butoxycarbonylmethoxyacetic Acid Benzyl Ester (30a). To a stirred solution of benzyl glycolate (2.34 g, 14.0 mmol) and rhodium acetate dimer (62 mg, 0.14 mmol) in CH₂-Cl₂ (20 mL) was added a solution of *tert*-butyl diazoacetate (2.01 g, 14.0 mmol) in CH₂Cl₂ (20.0 mL), via a syringe pump over 2.0 h. The reaction mixture was stirred overnight at room temperature, filtered through Celite, concentrated, and purified by flash chromatography (20% EtOAc/hexane) to afford **30a**, 2.40 g (61%). ¹H NMR (CDCl₃): δ 7.35 (m, 5H), 5.20 (s, 2H), 4.13 (s, 2H), 4.08 (s, 2H), 1.46 (s, 9H). MS (ES): 281 (M + H)⁺.

tert-Butoxycarbonylmethoxyacetic Acid (31). The reaction mixture composed of **30a** (1.0 g, 3.56 mmol) and 150 mg of 20% Pd(OH)₂/C (Pearlman's catalyst) in EtOAc (40 mL) was shaken on a Parr hydrogenator at 40 psi of H₂ for 8 h. It was then filtered through Celite and concentrated to yield **31**, 651 mg (96%). ¹H NMR (CD₃OD): δ 4.11 (s, 2H), 4.04 (s, 2H), 1.43 (s, 9H). MS (ES): 191 (M + H)⁺.

{2-[2-(4-Cyanophenyl)-1-oxo-2,8-diazaspiro[4.5]dec-8-yl]-2-oxoethoxy}acetic Acid *tert*-Butyl Ester (32). The reaction mixture composed of **11** (70 mg, 0.274 mmol), **31** (70 mg, 0.368 mmol), HBTU (230 mg, 0.606 mmol), and DIEA (150 μL, 0.86 mmol) in anhyd DMF (5.0 mL) was stirred at room temperature for 20 h. Then the reaction mixture was partitioned between CH₂Cl₂/satd NaHCO₃. The combined CH₂Cl₂ extract was washed with brine, dried over Na₂SO₄, concentrated, and purified by flash chromatography to yield **32**, 96 mg (82%). ¹H NMR (CDCl₃): δ 7.78 (d, 2H), 7.63 (d, 2H), 4.15–4.35 (m, 5H), 4.0 (m, 1H), 3.82 (m, 2H), 3.2–3.4 (m, 2H), 2.13 (q, 2H), 1.95 (m, 2H), 1.59 (m, 2H), 1.46 (s, 9H). MS (ES): 428 (M + H)⁺.

{2-[2-(4-Carbamimidoylphenyl)-1-oxo-2,8-diazaspiro[4.5]dec-8-yl]-2-oxoethoxy}acetic Acid (33) (CT51907). The compound **33** was synthesized from **32** by using Typical Procedure A, described previously for the synthesis of **21** from **20**, followed by deprotection of the *tert*-butyl ester functionality by treating with neat TFA, concentration, and RP-HPLC purification to yield as its HCl salt. Overall yield, 68%. ¹H NMR (CD₃OD): δ 7.93 (d, 2H), 7.70 (d, 2H), 4.34 (m, 2H), 4.24 (m, 1H), 4.14 (m, 2H), 3.92 (m, 3H), 3.34 (m, 1H), 3.10 (m, 1H), 2.14 (m, 2H), 1.8 (m, 2H), 1.60 (m, 4H). MS (ES): 389 (M + H)⁺. Exact mass (FAB, M + 1)⁺ calcd, 389.1819; found, 389.1731.

{2-[2-(4-Cyanophenyl)-1-oxo-2,8-diazaspiro[4.5]dec-8-yl]-2-oxoethoxy}acetic Acid Ethyl Ester (35). A mixture of **11** (225 mg, 0.881 mmol), **34** (172 mg, 1.061 mmol), HBTU (435 mg, 1.147 mmol), and DIEA (400 μL, 2.29 mmol) in DMF (5.0 mL) was stirred at room temperature for 6 h. Then it was partitioned between CH₂Cl₂/satd NaHCO₃ (3 ×). The combined CH₂Cl₂ extract was washed with brine, dried over Na₂SO₄, concentrated, and purified by flash chromatography to afford **35**, 306 mg (87%). ¹H NMR (CDCl₃): δ 7.78 (d, 2H), 7.63 (d, 2H), 4.15–4.35 (m, 7H), 4.0 (m, 1H), 3.82 (m, 2H), 3.2–3.4 (m, 2H), 2.13 (q, 2H), 1.95 (m, 2H), 1.59 (m, 2H), 1.37 (t, 3H). MS (ES): 400 (M + H)⁺.

(2-[2-[4-(N-Hydroxycarbamimidoyl)phenyl]-1-oxo-2,8-diazaspiro[4.5]dec-8-yl]-2-oxoethoxy)acetic Acid Ethyl Ester Hydrochloride (36) (CT052108). **35** (43 mg, 0.108 mmol) in EtOH (3.0 mL) at room temperature was treated with Et₃N (125 μL, 0.896 mmol), followed by hydroxylamine hydrochloride (33.0 mg, 0.47 mmol), and the mixture was stirred overnight at room temperature. Then it was concentrated under reduced pressure and purified by RP-HPLC to afford **36** as its HCl salt, 42 mg (83%). ¹H NMR (CD₃OD): δ 7.93 (d, 2H), 7.71 (d, 2H), 4.15–4.4 (m, 8H), 3.93 (q, 2H), 3.32 (m, 1H), 3.11 (m, 1H), 2.25 (m, 2H), 1.8 (m, 2H), 1.65 (m, 2H), 1.25 (t, 3H). MS (ES): 433 (M + H)⁺. Exact mass (FAB, M + 1)⁺ calcd, 433.2081; found, 433.2086.

(2-[2-[4-(N-Hydroxycarbamimidoyl)phenyl]-1-oxo-2,8-diazaspiro[4.5]dec-8-yl]-2-oxoethoxy)acetic Acid (37). **36** (16.0 mg, 0.034 mmol) was treated with 3 N HCl (1.0 mL), and the mixture was stirred at room temperature for 3 h. Then it was purified by RP-HPLC to afford **37**, 13 mg (86%). ¹H NMR (CD₃OD): δ 7.88 (d, 2H), 7.66 (d, 2H), 4.33 (d, 2H), 4.24 (m, 1H), 3.89 (q, 3H), 3.29 (m, 1H), 3.11 (m, 1H), 2.20 (m, 2H), 1.79–1.92 (m, 2H), 1.62 (m, 2H). MS (ES): 405 (M + H)⁺. Exact mass (FAB, M + 1)⁺ calcd, 405.1768; found, 405.1775.

5-[2-[4-(N-Ethylcarbamimidoyl)phenyl]-1-oxo-2,8-diazaspiro[4.5]dec-8-yl]-5-oxopentanoic Acid (40b). **40b** was synthesized using Typical Procedure B. (a). The benzonitrile **25** (36 mg, 0.090 mmol) was converted to thiomethylimide **38** by Typical Procedure A, described previously for the synthesis of **21**. (b). EtNH₂ (2.0 M/THF) (1.0 mL, 2.0 mmol) in MeOH (2.0 mL) was treated with AcOH (230 μL, 4.0 mmol). Then this mixture was added to thiomethyl imide **38** (0.090

mmol). After a stirring of 15 h at room temperature, the reaction mixture was concentrated, and purified by RP-HPLC to afford **40a**, 5-[2-[4-(*N*-Ethylcarbamimidoyl)-phenyl]-1-oxo-2,8-diazaspiro[4.5]dec-8-yl]-5-oxopentanoic acid ethyl ester, TFA salt, 39 mg (77% overall). (c). **40a** (34 mg, 0.061 mmol) was treated with 3 N HCl (1.0 mL) and the reaction mixture was stirred at room temperature for 8 h. Then it was concentrated, and purified by RP-HPLC to afford **40b**, 29 mg (90%), as a colorless solid. ¹H NMR (CD₃OD): δ 7.84 (d, 2H), 7.68 (d, 2H), 4.25 (m, 1H), 3.87 (m, 3H), 3.40 (m, 2H), 3.29 (m, 1H), 3.01 (m, 1H), 2.41 (m, 2H), 2.30 (m, 2H), 2.17 (m, 2H), 1.65–1.8 (m, 5H), 1.57 (m, 2H), 1.28 (t, 2H). MS (ES): 415 (M + H)⁺. Exact mass (FAB, M + 1)⁺ calcd, 415.2267; found, 415.2285.

5-[2-[4-(Iminomorpholin-4-ylmethyl)phenyl]-1-oxo-2,8-diazaspiro[4.5]dec-8-yl]-5-oxopentanoic Acid Ethyl Ester (39a). **39a** was synthesized from **38** using Typical Procedure B. Morpholine (35 μL, 0.40 mmol) in MeOH (1.0 mL) was treated with AcOH (50 μL, 0.87 mmol). This clear solution was then added to thiomethylimidate **38** (0.10 mmol, prepared from 0.10 mmol of **25**). The reaction mixture was stirred at room temperature for 20 h, concentrated, and purified by RP-HPLC to afford **39a**, as its TFA salt, 49 mg (82%). ¹H NMR (CD₃OD): δ 7.93 (d, 2H), 7.60 (d, 2H), 4.30 (m, 1H), 4.09 (q, 2H), 3.93 (m, 3H), 3.89 (m, 2H), 3.78 (t, 2H), 3.72 (t, 2H), 3.49 (t, 2H), 3.35 (m, 1H), 3.07 (m, 1H), 2.46 (m, 2H), 2.39 (t, 2H), 2.24 (m, 2H), 1.89 (m, 2H), 1.78 (m, 2H), 1.63 (m, 2H), 1.21 (t, 3H). MS (ES): 485 (M + H)⁺. Exact mass (FAB, M + 1)⁺ calcd, 485.2758; found, 485.2775.

5-[2-[4-(Iminomorpholin-4-ylmethyl)phenyl]-1-oxo-2,8-diazaspiro[4.5]dec-8-yl]-5-oxopentanoic Acid (39b). **39b** was synthesized from **39a** by the procedure described above for the synthesis of **40b** from **40a**, to yield **39b** as its TFA salt, 40 mg (86%). ¹H NMR (CD₃OD): δ 7.86 (d, 2H), 7.52 (d, 2H), 4.23 (m, 1H), 3.85 (m, 3H), 3.71 (t, 2H), 3.66 (t, 2H), 3.30 (m, 1H), 3.01 (m, 1H), 2.41 (m, 2H), 2.32 (m, 2H), 2.19 (t, 2H), 1.80 (m, 2H), 1.73 (m, 2H), 1.59 (m, 2H). MS (ES): 457 (M + H)⁺. Exact mass (FAB, M + 1)⁺ calcd, 457.2445; found, 457.2459.

3-(*R*)-Methylpentanedioic Acid *tert*-Butyl Ester Ethyl Ester (41). The reaction mixture comprised of (*R*)-1-ethyl hydrogen-3-methylglutarate (1.0 g, 5.74 mmol), *tert*-butyl alcohol (4.30 g, 58.0 mmol), DMAP (250 mg, 2.046 mmol), and DCC (1.50 g, 7.27 mmol) in CH₂Cl₂ (10 mL) was stirred at room temperature for 20 h. Then it was partitioned between CH₂Cl₂/satd NaHCO₃. The combined CH₂Cl₂ extract was washed with brine, dried over Na₂SO₄, concentrated, and purified by flash chromatography (CH₂Cl₂/MeOH) to yield **41**, 1.10 g (83%). MS (ES): 231 (M + H)⁺.

3-(*S*)-Methylpentanedioic Acid Mono-*tert*-butyl Ester (42). Compound **41** (1.20 g, 4.647 mmol) in THF (40 mL) was treated with 1 M LiOH (10 mL, 10.0 mmol), and the mixture was stirred at room temperature for 18 h. It was acidified at 0 °C with AcOH (2.0 mL), and partitioned between EtOAc/brine. The combined EtOAc extract was washed with brine, dried over Na₂SO₄, concentrated, and purified by flash chromatography (CH₂Cl₂/MeOH) to afford **42**, 854 mg (81%). MS (ES): 203 (M + H)⁺.

5-[2-(4-Cyanophenyl)-1-oxo-2,8-diazaspiro[4.5]dec-8-yl]-3-(*S*)-methyl-5-oxopentanoic Acid *tert*-Butyl Ester (43). The reaction mixture comprised of **11** (70.0 mg, 0.274 mmol), **42** (80 mg, 0.395 mmol), HBTU (230 mg, 0.606 mmol), and DIEA (0.150 mL, 0.86 mmol) in DMF (2.0 mL) was stirred at room temperature for 17 h. Then it was partitioned between CH₂Cl₂/satd NaHCO₃. The combined CH₂Cl₂ extract was washed with brine, dried over Na₂SO₄, concentrated, and purified by flash chromatography (CH₂Cl₂/MeOH) to yield **43**, 103 mg (86%). MS (ES): 440 (M + H)⁺.

5-[2-(4-Carbamidoylphenyl)-1-oxo-2,8-diazaspiro[4.5]dec-8-yl]-3-(*S*)-methyl-5-oxopentanoic Acid (44). Compound **44** was synthesized from **43**, by Typical Procedure A, described previously for the synthesis of **21** from **20**, followed by deprotection of the *tert*-butyl ester functionality by treatment with neat TFA, in 67% overall yield. ¹H NMR (CD₃OD):

δ 7.86 (d, 2H), 7.72 (d, 2H), 4.23 (m, 1H), 3.9 (m, 3H), 3.3 (m, 1H), 3.01 (m, 1H), 2.46 (m, 2H), 2.1–2.4 (m, 5H), 1.77 (m, 2H), 1.58 (m, 2H), 0.97 (d, 3H). MS (ES): 401 (M + H)⁺. Exact mass (FAB, M + 1)⁺ calcd, 401.2183; found, 401.2142.

5-[2-(4-Carbamidoylphenyl)-1-oxo-2,8-diazaspiro[4.5]dec-8-yl]-3-(*R*)-methyl-5-oxopentanoic Acid (45). Compound **45** was synthesized starting from (*R*)-1-ethyl-hydrogen-3-methyl glutarate and **11** by the procedures described above for the synthesis of **44**, in 71% overall yield. ¹H NMR (CD₃OD): δ 7.86 (d, 2H), 7.72 (d, 2H), 4.18 (m, 1H), 3.9 (m, 3H), 3.3 (m, 1H), 3.01 (m, 2H), 2.54 (d, 1H), 2.40 (d, 1H), 2.21 (t, 2H), 1.83 (m, 2H), 1.56 (m, 2H), 1.2 (d, 3H). MS (ES): 401 (M + H)⁺. Exact mass (FAB, M + 1)⁺ calcd, 401.2183; found, 401.2156.

3-Phenylpentanedioic Acid Monoethyl Ester (46). 3-Phenylglutaric acid (1.0 g, 4.80 mmol) was suspended in Ac₂O (20.0 mL), and the reaction mixture was refluxed for 15 h. Then it was concentrated under reduced pressure to afford 3-phenylglutaric anhydride.

This was dissolved in EtOH (30.0 mL), Et₃N (3.0 mL, 21.52 mmol) was added, and the mixture was stirred at room temperature for 20 h. Then it was concentrated and purified by flash chromatography (40% EtOAc/hexane) to afford **46**, 984 mg (87%). ¹H NMR (CD₃OD): δ 7.24 (m, 5H), 3.96 (q, 2H), 3.53 (m, 1H), 2.5–2.8 (m, 4H), 1.08 (t, 3H). MS (ES): 237 (M + H)⁺.

5-[2-(4-Cyanophenyl)-1-oxo-2,8-diazaspiro[4.5]dec-8-yl]-5-oxo-3-phenylpentanoic Acid Ethyl Ester (47). The reaction mixture composed of **11** (90 mg, 0.352 mmol), **46** (110 mg, 0.465 mmol), EDC·HCl (160 mg, 0.834 mmol), and HOBT (95 mg, 0.70 mmol) in anhyd DMF (4.0 mL) was stirred at room temperature for 20 h. Then it was partitioned between CH₂Cl₂/satd NaHCO₃. The combined CH₂Cl₂ extract was washed with brine, dried over Na₂SO₄, concentrated, and purified by flash chromatography (CH₂Cl₂/MeOH) to afford **47**, 149 mg (89%). ¹H NMR (CDCl₃): δ 7.76 (d, 2H), 7.60 (d, 2H), 7.18 (m, 5H), 4.05–4.25 (m, 2H), 3.98 (q, 2H), 3.79 (m, 3H), 3.68 (m, 1H), 3.16 (m, 2H), 2.81 (m, 1H), 2.64 (m, 4H), 2.05 (m, 2H), 1.8 (m, 2H), 1.09 (t, 3H). MS (ES): 474 (M + H)⁺.

5-[2-(4-Carbamidoylphenyl)-1-oxo-2,8-diazaspiro[4.5]dec-8-yl]-5-oxo-3-phenylpentanoic Acid (48). Compound **48** was synthesized from **47** by using the procedures described previously for the synthesis of **23** from **20**, in overall yield of 64%. ¹H NMR (CD₃OD): δ 7.92 (d, 2H), 7.8 (d, 2H), 7.2 (m, 5H), 4.2 (m, 1H), 3.92 (m, 3H), 3.58 (m, 1H), 2.9–3.25 (m, 2H), 2.6–2.8 (m, 4H), 2.10 (m, 2H), 1.2–1.8 (m, 4H). MS (ES): 463 (M + H)⁺. Exact mass (FAB, M + 1)⁺ calcd, 463.2267; found, 463.2288.

3-(4-Nitro-phenoxy-carbonylamino)-butyric Acid Ethyl Ester (51). Ethyl 3-(*R*)-methyl-β-alanine (**50**) (1.0 g, 7.623 mmol) in CH₂Cl₂ (20.0 mL) was treated with DIEA (3.0 mL, 17.22 mmol), followed by 4-nitrophenyl chloroformate (2.0 g, 9.922 mmol), and the mixture was stirred at room temperature for 9 h. Then it was partitioned between CH₂Cl₂/satd NaHCO₃. The combined CH₂Cl₂ extract was washed with brine, dried over Na₂SO₄, concentrated, and purified by flash chromatography to afford **51**, 1.96 g (87%). ¹H NMR (CDCl₃): δ 8.22 (d, 2H), 7.30 (d, 2H), 5.84 (s, 1H), 4.16 (m, 3H), 2.60 (m, 2H), 1.33 (d, 3H), 1.26 (t, 3H). MS (ES): 297 (M + H)⁺.

3-[(2-(4-Cyanophenyl)-1-oxo-2,8-diazaspiro[4.5]decane-8-carbonyl)amino]-butyric Acid Ethyl Ester (52). **11** (500 mg, 1.958 mmol) in CH₂Cl₂ (10.0 mL) was treated with DIEA (0.700 mL, 4.02 mmol), followed by **51** (750 mg, 2.531 mmol), and the reaction mixture was stirred overnight at room temperature. Then it was partitioned between CH₂Cl₂/satd NaHCO₃. The combined CH₂Cl₂ extract was washed with brine, dried over Na₂SO₄, concentrated, and purified by flash chromatography to afford **52**, 687 mg (85%). ¹H NMR (CDCl₃): δ 7.78 (d, 2H), 7.63 (d, 2H), 5.7 (s, 1H), 4.23 (m, 1H), 4.12 (m, 2H), 3.83 (m, 4H), 3.12 (m, 2H), 2.51 (m, 2H), 2.12 (m, 2H), 1.96 (m, 2H), 1.56 (m, 2H), 1.2 (m, 6H). MS (ES): 413 (M + H)⁺.

3-[(2-(4-Carbamidoylphenyl)-1-oxo-2,8-diazaspiro[4.5]decane-8-carbonyl)amino]-butyric Acid (53). Com-

pound **53** was synthesized from **52** by using Typical Procedure A, described previously for the synthesis of **23** from **20**, in overall yield of 70%. ¹H NMR (CD₃OD): δ 7.9 (d, 2H), 7.78 (d, 2H), 4.14 (m, 1H), 3.88 (m, 4H), 3.04 (m, 2H), 2.48 (m, 1H), 2.38 (m, 1H), 2.18 (d, 2H), 1.79 (m, 2H), 1.53 (d, 2H), 1.15 (m, 3H). MS (ES): 402 (M + H)⁺. Exact mass (FAB, M + 1)⁺ calcd, 402.2135; found, 402.2160.

3-(4-Nitro-phenoxycarbonylamino)-3-phenylpropionic Acid Ethyl Ester (54). 3-Amino-3-phenylpropionic acid ethyl ester (1.0 g, 5.175 mmol) was converted to its 4-nitrophenyl carbamate **54** by using the procedure described previously for the synthesis of **51** from **50**. Yield, 1.54 g (83%). ¹H NMR (CDCl₃): δ 8.21 (d, 2H), 7.3 (m, 7H), 6.31 (d, 1H), 5.22 (m, 1H), 4.1 (q, 2H), 2.93 (m, 2H), 1.18 (t, 3H). MS (ES): 359 (M + H)⁺.

3-{[3-(4-Cyanophenyl)-1-methyl-2,4-dioxo-1,3,8-triazaspiro[4.5]decane-8-carbonyl]amino}-3-phenylpropionic Acid Ethyl Ester (55). Compound **55** was synthesized in 79% overall yield from **54** (160 mg, 0.446 mmol) and **19b** (100 mg, 0.351 mmol) by using the procedure described previously for the synthesis of **52**. ¹H NMR (CD₃OD): δ 7.8 (d, 2H), 7.62 (d, 2H), 7.35 (d, 2H), 7.3 (d, 2H), 7.2 (m, 1H), 5.3 (dd, 1H), 4.05 (m, 4H), 3.4–3.6 (m, 2H), 2.90 (s, 3H), 2.7–2.85 (m, 2H), 1.95–2.1 (m, 2H), 1.85 (d, 2H), 1.09 (t, 3H). MS (ES): 504 (M + H)⁺.

3-{[3-(4-Carbamidoylphenyl)-1-methyl-2,4-dioxo-1,3,8-triazaspiro[4.5]decane-8-carbonyl]amino}-3-phenylpropionic Acid (56). Compound **56** was synthesized from **55** by using Typical Procedure A, described previously for the synthesis of **23** from **20**, in overall yield 69%. ¹H NMR (CD₃OD): δ 7.9 (d, 2H), 7.7 (d, 2H), 7.35 (d, 2H), 7.3 (d, 2H), 7.2 (m, 1H), 5.3 (dd, 1H), 4.05 (t, 2H), 3.4–3.6 (m, 2H), 2.90 (s, 3H), 2.7–2.85 (m, 2H), 1.95–2.1 (m, 2H), 1.85 (d, 2H). MS (ES): 493 (M + H)⁺. Exact mass (FAB, M + 1)⁺ calcd, 493.2121; found, 493.2146.

2-(3,5-Dimethylisoxazole-4-sulfonylamino)pentanedioic Acid 1-tert-Butyl Ester (57). L-Glutamic acid α-tert-butyl ester (1.0 g, 4.92 mmol) was dissolved in 1 N NaOH (5.0 mL, 5.0 mmol), diluted with H₂O (50 mL), and cooled to 0 °C. Then Na₂CO₃ (583 mg, 5.50 mmol) was added, followed by 3,5-dimethylisoxazole-4-sulfonyl chloride (1.06 g, 5.418 mmol), and the mixture was stirred at room temperature for 20 h. Then it was acidified with 2 N HCl at 0 °C to pH 3 and extracted with EtOAc (3 ×). The combined EtOAc extract was washed with brine, dried over Na₂SO₄, concentrated, and purified by RP-HPLC to afford **57**, 1.57 g (88%). ¹H NMR (CDCl₃): δ 3.75 (m, 1H), 2.60 (s, 3H), 2.54 (m, 1H), 2.39 (s, 3H), 2.08 (m, 1H), 1.84 (m, 1H), 1.32 (s, 9H). MS (ES): 363 (M + H)⁺.

5-[2-(4-Cyanophenyl)-1-oxo-2,8-diazaspiro[4.5]dec-8-yl]-2-(3,5-dimethylisoxazole-4-sulfonylamino)-5-oxopentanoic Acid tert-Butyl Ester (58). The reaction mixture composed of **11** (25.0 mg, 0.0979 mmol), **57** (42 mg, 0.116 mmol), and EDC·HCl (37.0 mg, 0.193 mmol) in DMF (2.0 mL) was stirred at room temperature for 18 h. Then it was partitioned between CH₂Cl₂/satd NaHCO₃. The combined CH₂Cl₂ extract was washed with brine, dried over Na₂SO₄, concentrated, and purified by flash chromatography (CH₂Cl₂/MeOH) to afford **58**, 53 mg (90%). ¹H NMR (CD₃OD): δ 7.95 (d, 2H), 7.80 (d, 2H), 4.25 (m, 1H), 3.95 (m, 4H), 3.35 (m, 1H), 3.13 (q, 1H), 2.58 (m, 4H), 2.38 (s, 3H), 2.22 (t, 2H), 1.6–2.0 (m, 7H), 1.43 (s, 9H). MS (ES): 600 (M + H)⁺.

5-[2-(4-Carbamidoylphenyl)-1-oxo-2,8-diazaspiro[4.5]dec-8-yl]-2-(3,5-dimethylisoxazole-4-sulfonylamino)-5-oxopentanoic Acid (59) (CT50787). Compound **59** was synthesized from **58** using Typical Procedure A, described previously for the synthesis of **21** from **20**. Overall yield, 66%. ¹H NMR (CD₃OD): δ 7.95 (d, 2H), 7.80 (d, 2H), 4.25 (m, 1H), 3.95 (m, 4H), 3.35 (m, 1H), 3.13 (q, 1H), 2.58 (m, 4H), 2.38 (s, 3H), 2.22 (t, 2H), 1.6–2.0 (m, 7H). MS (ES): 561 (M + H)⁺. Exact mass (FAB, M + 1)⁺ calcd, 561.2125; found, 561.2120.

3-tert-Butoxycarbonylamino-2-(toluene-4-sulfonylamino)propionic Acid Ethyl Ester (60). 2-L-Amino-3-tert-butoxycarbonylamino propionic acid ethyl ester (2.0 g, 8.61 mmol) in CH₂Cl₂ (40 mL) at 0 °C was treated with DIEA (3.0

mL, 17.22 mmol), followed by tosyl chloride (1.64 g, 8.60 mmol), and stirred at room temperature for 2.0 h. Then the reaction mixture was partitioned between CH₂Cl₂/satd NaHCO₃. The combined CH₂Cl₂ extract was washed with brine, dried over Na₂SO₄, concentrated, and purified by flash chromatography (CH₂Cl₂/MeOH) to yield **60**, 2.30 g (69%). ¹H NMR (CDCl₃): δ 7.70 (d, 2H), 7.28 (d, 2H), 5.50 (d, 1H), 4.9 (m, 1H), 3.95 (m, 3H), 3.44 (m, 2H), 2.39 (s, 1H), 1.41 (s, 9H), 1.11 (t, 2H). MS (ES): 387 (M + H)⁺.

3-Amino-2-(toluene-4-sulfonylamino)propionic Acid Ethyl Ester (61). **60** (1.72 g, 4.45 mmol) was treated with anhyd TFA (15.0 mL) at room temperature. After 2.0 h the reaction mixture was concentrated to dryness, and partitioned between EtOAc/satd NaHCO₃. The EtOAc extract was washed with brine, dried over Na₂SO₄, and concentrated to yield **61**, 1.02 g (90%). ¹H NMR (CDCl₃): δ 7.71 (d, 2H), 7.27 (d, 2H), 3.98 (q, 2H), 3.86 (m, 1H), 2.95–3.05 (m, 2H), 2.40 (s, 3H), 1.10 (t, 3H). MS (ES): 287 (M + H)⁺.

3-[2-(4-Cyanophenyl)-1-oxo-2,8-diazaspiro[4.5]decane-8-carbonyl]amino-2-(toluene-4-sulfonylamino)propionic Acid Ethyl Ester (62). A mixture of **11** (28.0 mg, 0.109 mmol) and DIEA (80 μL, 0.46 mmol) in CH₂Cl₂ (3.0 mL) was added dropwise to a solution of triphosgene (12.0 mg, 0.0404 mmol) in CH₂Cl₂ (2.0 mL) at 0 °C, and the mixture was stirred at 0 °C for 0.5 h. Then was added a solution of **61** (33.0 mg, 0.13 mmol) in CH₂Cl₂ (1.0 mL), and the mixture was stirred overnight at room temperature. Then it was partitioned between CH₂Cl₂/satd NaHCO₃, and CH₂Cl₂ extract was washed with brine, dried over Na₂SO₄, concentrated, and purified by prep-TLC (5% MeOH/CH₂Cl₂) to afford **62**, 40 mg (64%). ¹H NMR (CDCl₃): δ 7.79 (d, 2H), 7.69 (d, 2H), 7.63 (d, 2H), 7.28 (d, 2H), 5.77 (d, 1H), 5.14 (t, 1H), 4.01 (q, 2H), 3.8–3.95 (m, 2H), 3.82 (t, 2H), 3.68–3.76 (m, 2H), 3.3–3.45 (m, 1H), 3.2–3.3 (m, 1H), 3.03 (m, 1H), 2.40 (s, 3H), 2.13 (t, 2H), 1.85–2.0 (m, 2H), 1.5–1.65 (m, 2H), 1.12 (t, 3H). MS (ES): 568 (M + H)⁺.

3-[2-(4-Carbamidoylphenyl)-1-oxo-2,8-diazaspiro[4.5]decane-8-carbonyl]amino-2-(toluene-4-sulfonylamino)propionic Acid (63). Compound **63** was synthesized from **62** by using Typical Procedure C. (a) **62** (48.0 mg, 0.0845 mmol) in EtOH (2.0 mL) was treated with Et₃N (60 μL, 0.430 mmol), followed by hydroxylamine hydrochloride (24.0 mg, 0.345 mmol). The reaction mixture was heated to 50 °C for 8.0 h and then partitioned between CH₂Cl₂/brine. The CH₂Cl₂ extract was dried over Na₂SO₄ and concentrated to afford 3-({2-[4-(N-Hydroxycarbamidoyl)-phenyl]-1-oxo-2,8-diazaspiro[4.5]decane-8-carbonyl}amino)-2-(toluene-4-sulfonylamino)propionic acid ethyl ester, 35 mg (69%). (b) This was then dissolved in acetic acid (1.0 mL), treated with acetic anhydride (12.0 μL, 0.127 mmol), and stirred at room temperature for 0.5 h. Then 10% Pd/C (10.0 mg) was added, and the reaction mixture was stirred under 1 atm H₂ pressure (balloon) for 3.0 h. The mixture was filtered through Celite and concentrated to afford 3-[2-(4-carbamimidoylphenyl)-1-oxo-2,8-diazaspiro[4.5]decane-8-carbonyl]amino-2-(toluene-4-sulfonylamino)propionic acid ethyl ester. (c) This was then dissolved in THF (5.0 mL), treated with 1 M LiOH (1.0 mL, 1.0 mmol), and the mixture was stirred at room temperature for 14 h. The reaction mixture was acidified with 6N HCl, concentrated to dryness, and purified by RP-HPLC to afford **63** as a colorless solid as its TFA salt, 43 mg (76% overall). ¹H NMR (CD₃OD): δ 7.96 (d, 2H), 7.83 (d, 2H), 7.71 (d, 2H), 7.34 (d, 2H), 4.0 (dd, 1H), 3.93 (t, 2H), 3.84 (m, 2H), 3.51 (dd, 1H), 3.1 (t, 2H), 2.42 (s, 3H), 2.20 (t, 2H), 1.82 (m, 2H), 1.59 (d, 2H), 1.36 (dd, 1H). MS (ES): 557 (M + H)⁺. Exact mass (FAB, M + 1)⁺ calcd, 557.2176; found, 557.2207.

2-Benzyloxycarbonylamino pentanedioic Acid 5-tert-Butyl Ester 1-Ethyl Ester (64). The reaction mixture, consisting of Z-Glu (O-*t*-Bu)-OH (5.0 g, 14.82 mmol), EtOH (8.75 mL, 150 mmol), EDC·HCl (6.53 g, 34.06 mmol), and HOBt (4.53 g, 33.52 mmol) in DMF (50 mL) was stirred at room temperature for 16 h. Then it was partitioned between CH₂Cl₂/satd NaHCO₃, the CH₂Cl₂ extract was washed with brine, dried over Na₂SO₄, concentrated, and purified by flash

chromatography (5% MeOH/CH₂Cl₂) to yield **64**, 4.47 g (83%). ¹H NMR (CDCl₃): δ 7.3 (m, 5H), 5.42 (d, 1H), 5.06 (s, 2H), 4.34 (m, 1H), 4.15 (q, 2H), 2.27 (m, 2H), 2.11 (m, 1H), 1.90 (m, 1H), 1.4 (s, 9H), 1.23 (t, 3H). MS (ES): 366 (M + H)⁺.

2-Aminopentanedioic Acid 5-tert-Butyl Ester 1-Ethyl Ester (65). **64** (4.47 g, 12.23 mmol) in EtOH (60 mL) was mixed with 20% Pd(OH)₂/C (250 mg), and the mixture was shaken on a Parr hydrogenator under 50 psi H₂ for 7 h. Then it was filtered through Celite and concentrated to yield **65**, 2.58 g (91%). ¹H NMR (CDCl₃): δ 4.05 (q, 2H), 3.60 (s, 1H), 3.32 (m, 1H), 2.23 (t, 2H), 1.91 (m, 1H), 1.58 (m, 1H), 1.33 (s, 9H), 1.15 (t, 3H). MS (ES): 232 (M + H)⁺.

2-Butoxycarbonylamino-pentanedioic Acid 5-tert-Butyl Ester 1-Ethyl Ester (66). To a solution of **65** (2.58 g, 11.15 mmol) in CH₂Cl₂ (50 mL) at 0 °C was added DIEA (3.90 mL, 22.39 mmol), followed by butyl chloroformate (1.87 mL, 14.70 mmol) in CH₂Cl₂ (5.0 mL). The reaction mixture was stirred at room temperature for 20 h. Then it was partitioned between CH₂Cl₂/satd NaHCO₃, and the CH₂Cl₂ extract was washed with brine, dried over Na₂SO₄, concentrated, and purified by flash chromatography (CH₂Cl₂/MeOH) to yield **66**, 3.18 g (86%). ¹H NMR (CDCl₃): δ 4.30 (m, 1H), 4.15 (q, 2H), 4.02 (t, 2H), 2.28 (m, 2H), 2.09 (m, 1H), 1.88 (m, 1H), 1.54 (m, 2H), 1.39 (s, 9H), 1.32 (m, 2H), 1.24 (t, 3H), 0.94 (t, 3H). MS (ES): 332 (M + H)⁺.

2-Butoxycarbonylamino-pentanedioic Acid 1-Ethyl Ester (67). **66** (2.61 g, 7.875 mmol) was treated with TFA (20.0 mL), and the mixture was stirred at room temperature for 5.0 h, then concentrated to yield **67**, 2.08 g (96%). ¹H NMR (CDCl₃): δ 4.35 (m, 1H), 4.15 (q, 2H), 4.02 (t, 2H), 2.42 (m, 2H), 2.15 (m, 1H), 1.84 (m, 1H), 1.57 (m, 2H), 1.18–1.4 (m, 5H), 0.87 (t, 3H). MS (ES): 276 (M + H)⁺.

2-Butoxycarbonylamino-5-[2-(4-cyanophenyl)-1-oxo-2,8-diazaspiro[4.5]dec-8-yl]-5-oxopentanoic Acid Ethyl Ester (68). The reaction mixture consisting of **11** (98 mg, 0.383 mmol), **67** (127 mg, 0.46 mmol), HBTU (218 mg, 0.575 mmol), and DIEA (150 μL, 0.86 mmol) in DMF (3.0 mL) was stirred at room temperature for 17 h. Then it was partitioned between CH₂Cl₂/satd NaHCO₃, the CH₂Cl₂ extract was washed with brine, dried over Na₂SO₄, concentrated, and purified by flash chromatography (5% MeOH/CH₂Cl₂) to yield **68**, 167 mg (85%). ¹H NMR (CD₃OD): δ 7.73 (d, 2H), 7.56 (d, 2H), 4.3 (m, 1H), 4.2 (m, 3H), 4.04 (t, 2H), 3.84 (t, 1H), 3.1–3.4 (m, 3H), 2.55 (m, 2H), 2.25 (m, 2H), 1.85–2.05 (m, 2H), 1.75–1.85 (m, 2H), 1.6 (m, 2H), 1.4 (m, 2H), 1.28 (m, 2H), 0.93 (t, 3H). MS (ES): 513 (M + H)⁺.

2-Butoxycarbonylamino-5-[2-(4-carbamimidoylphenyl)-1-oxo-2,8-diazaspiro[4.5]dec-8-yl]-5-oxopentanoic Acid (69). **69** was synthesized from **68** by Typical Procedure C, described previously for the synthesis of **63** from **62**. Overall yield, 68%. ¹H NMR (CD₃OD): δ 7.95 (d, 2H), 7.85 (d, 2H), 4.3 (m, 1H), 4.18 (m, 1H), 4.04 (t, 2H), 3.84 (t, 1H), 3.1–3.4 (m, 3H), 2.55 (m, 2H), 2.25 (m, 2H), 1.85–2.05 (m, 2H), 1.75–1.85 (m, 2H), 1.6 (m, 2H), 1.4 (m, 2H), 1.28 (m, 2H), 0.93 (t, 3H). MS (ES): 502 (M + H)⁺. Exact mass (FAB, M + 1)⁺ calcd, 502.2660; found, 502.2701.

5-[2-(4-Cyanophenyl)-1-oxo-2,8-diazaspiro[4.5]dec-8-yl]-pentanoic Acid Ethyl Ester (70). The reaction mixture consisting of **11** (160 mg, 0.626 mmol), ethyl 5-bromovaleate (130 μL, 0.821 mmol), and DIEA (0.400 mL, 2.29 mmol) in DMF (2.0 mL) was stirred overnight at room temperature. Then it was partitioned between CH₂Cl₂/satd NaHCO₃. The combined CH₂Cl₂ extract was washed with brine, dried over Na₂SO₄, concentrated, and purified by flash chromatography (CH₂Cl₂/MeOH) to afford **70**, 174 mg (73%). ¹H NMR (CDCl₃): δ 7.80 (d, 2H), 7.62 (d, 2H), 4.10 (q, 2H), 3.76 (t, 2H), 2.86 (m, 2H), 2.32 (m, 4H), 2.03 (m, 6H), 1.63 (m, 2H), 1.5 (m, 4H), 1.24 (t, 3H). MS (ES): 384 (M + H)⁺.

5-[2-(4-Carbamimidoylphenyl)-1-oxo-2,8-diazaspiro[4.5]dec-8-yl]pentanoic Acid (72). **72** was synthesized from **70** by using Typical Procedure C described for the synthesis of **63** from **62**. Yield, 66 mg (65%). ¹H NMR (CD₃OD): δ 7.98 (d, 2H), 7.82 (d, 2H), 3.96 (m, 1H), 3.63 (m, 1H), 3.45 (m, 1H), 3.10 (m, 4H), 2.4 (t, 2H), 2.3 (m, 2H), 2.13 (m, 2H), 1.9 (m,

3H), 1.80 (m, 2H), 1.66 (m, 2H). MS (ES): 373 (M + H)⁺. Exact mass (FAB, M + 1)⁺ calcd, 373.2234; found, 373.2272.

2,2-Dimethyl-3-(4-nitrophenoxycarbonyloxy)propionic Acid Methyl Ester (73). Methyl 2,2-dimethyl-3-hydroxypropionate (1.26 g, 9.53 mmol) in CH₂Cl₂ (40.0 mL) at 0 °C was treated with Et₃N (3.0 mL, 21.52 mmol), followed by 4-nitrophenyl chloroformate (2.50 g, 12.40 mmol). The reaction mixture was then stirred overnight at room temperature, washed with brine, dried over Na₂SO₄, concentrated, and purified by flash chromatography (20% CH₃CN/CH₂Cl₂) to afford **73**, 2.35 g (83%). ¹H NMR (CDCl₃): δ 8.24 (d, 2H), 7.36 (d, 2H), 4.30 (s, 2H), 3.71 (s, 3H), 1.3 (s, 6H). MS (ES): 298 (M + H)⁺.

2-(4-Cyanophenyl)-3-oxo-2,8-diazaspiro[4.5]decane-8-carboxylic Acid 2-Methoxycarbonyl-2-methylpropyl Ester (74). **12** (50 mg, 0.196 mmol) in DMF (2.0 mL) was treated with DIEA (70.0 μL, 0.40 mmol), followed by **73** (71 mg, 0.238 mmol), and the reaction mixture was stirred at room temperature for 18 h. Then it was partitioned between CH₂Cl₂/satd NaHCO₃, and the CH₂Cl₂ extract was washed with brine, dried over Na₂SO₄, concentrated, and purified by flash chromatography (3% MeOH/CH₂Cl₂) to afford **74**, 68 mg (84%). ¹H NMR (CDCl₃): δ 7.72 (d, 2H), 7.62 (d, 2H), 4.09 (s, 2H), 3.62 (m, 7H), 3.28 (m, 2H), 2.53 (s, 2H), 1.65 (m, 4H), 1.19 (s, 6H). MS (ES): 414 (M + H)⁺.

2-(4-Carbamimidoylphenyl)-3-oxo-2,8-diazaspiro[4.5]decane-8-carboxylic Acid 2-Carboxy-2-methylpropyl Ester (75). **75** was synthesized from **74** (27.0 mg, 0.065 mmol) by using Typical Procedure A, described previously for the synthesis of **56** from **55**. Yield, 23 mg of TFA salt (66%). ¹H NMR (CD₃OD): δ 7.78 (d, 2H), 7.67 (d, 2H), 3.90 (s, 2H), 3.64 (s, 2H), 3.42 (m, 2H), 3.23 (m, 2H), 2.43 (s, 2H), 1.45 (m, 4H), 1.03 (s, 6H). MS (ES): 417 (M + H)⁺. Exact mass (FAB, M + 1)⁺ calcd, 417.2132; found, 417.2096.

Pharmacology. In Vitro Assay Systems. All compounds were subjected to a series of functional in vitro assays to determine their relative activities. The following activities are expressed as the amount required to inhibit 50% of any given response (IC₅₀ values). Each compound was first tested for its ability to inhibit platelet aggregation induced by 20 μM ADP in citrated platelet rich plasma (PRP). If that IC₅₀ was <0.1 μM, the IC₅₀ was also obtained for most compounds with PPACK PRP using 20 μM ADP. If that criterion was met, then TRAP was tested as the agonist for comparison. In vitro fibrinogen binding to purified GPIIb-IIIa in a plate assay was also performed for the majority of the compounds and corresponding IC₅₀ values were obtained. Additionally, candidate compounds selected for further analysis were tested for their specificity for GPIIb-IIIa. This included analysis of inhibition of vitronectin (VN) binding to purified vitronectin receptor (VNR) in a plate assay and inhibition of cell adhesion mediated by various Integrins.

Materials and Methods (Platelet aggregation in platelet rich plasma). Materials: ADP diluted to 5 mL in PBS is 1 mM and prediluted Collagen are from Chrono-log Corp. TRAP6 (SFLLRN-NH2) was purchased from PenLabs, and TRAP 211–47 was synthesized in house at COR Therapeutics, Inc. 3.8% trisodium citrate (TSC) and PPACK (25 mg/mL in 0.01 N HCl, from CalBiochem) stock solutions were used. Fresh human blood was obtained from donors. Compounds were at a stock concentration of 40 mM in DMSO. Chrono-Log Whole Blood Aggregometer and Aggro-Link Software (Chrono-log corp., Havertown, PA) were used.

Procedure: Blood donors were selected who had not had any medications within the past 7 days and blood was drawn into 1/7 volume of TSC (8.6 mL TSC per 60 mL whole blood: final concentration: 0.54%) or PPACK (final concentration 0.3 mM). Ten milliliters of blood was aliquoted into 15 mL polypropylene tubes and centrifuged at 900 rpm for 20 min (160g). The platelet rich plasma (PRP) was carefully removed and pooled in a new tube. Platelet poor plasma (PPP), for the blank sample in the aggregometer, was obtained by pelleting platelets by centrifuging 2 × 600 μL aliquots of PRP for 5 min on high in a microfuge (15 000g).

The platelet aggregation procedure was as follows: 500 μ L of PRP was aliquoted into a cuvette with a stir bar, then 1 μ L of either vehicle or compound in vehicle was added. The aggregometer was set to zero, and sample was allowed to incubate while stirring for approximately 1 min. To initiate platelet aggregation, 10 μ L of 1 mM ADP was added to the cuvette for a final ADP concentration of 20 μ M ADP (or TRAP for a final concentration of 5 μ M). Aggregation proceeded for 5 min per sample. The amplitude value (height) of each aggregation curve, generated by the Aggro-Link Software, was used to generate inhibition curves for each compound. The IC₅₀ of each compound was calculated by linear regression using the two points that surround the 50% aggregation value. The average of at least three separate IC₅₀ determinations are reported here (\pm SD).

Fibrinogen Binding to Immobilized GPIIb-IIIa. (Protocol also used for vitronectin binding to VNR- α v β 3). Materials: Immulon-2 96-well microtiter plate. Biotinylated fibrinogen or vitronectin as per protocol (below). Buffer A: 0.15 M NaCl, 0.02 M Tris; pH 7.4, 0.001 M CaCl₂, 0.02% NaN₃. Buffer B: 0.1 M NaCl, 0.05 M Tris; pH 7.4, 0.002 M CaCl₂, 0.02% NaN₃. Buffer C: (blocking buffer): Buffer B with 35 mg/mL BSA. Buffer D: (Incubation Buffer): Buffer B with 1 mg/mL BSA. 0.4 N NaOH. Bovine serum albumin (BSA) (Sigma, St. Louis, MO).

Anti-biotin antibody-alkaline phosphatase conjugate (Sigma, St. Louis, MO. Product No. A-7064). Alkaline Phosphatase substrate kit (Biorad Laboratories, Hercules, CA. Cat No. 172-1063). V Max Plate Reader (Molecular Devices, Sunnyvale, CA).

Procedure: Purified GPIIb-IIIa complex or purified VNR was immobilized onto Immulon-2 96 well plates by diluting a 1 mg/ml stock 1:200 in buffer A and immediately adding 100 μ L to each well (0.5 μ g). The plates were incubated overnight at 4 °C. At the time of the experiment, the wells were washed twice with buffer B, by emptying then filling by aspiration. The wells were blocked with 0.1 mL of buffer C for 2 h at room temperature. The wells were washed with 250 μ L of buffer D and then the samples were added as follows: test compound and 10 nM biotinylated fibrinogen in buffer D were mixed together and 0.1 mL per well was added in triplicate. Following a 2 h incubation at room temperature, wells were washed once with 250 μ L buffer D and then 0.1 mL anti-biotin antibody (1:20 000 dilution in buffer D) was added and incubated for 1 h at room temperature. Wells were again washed with 250 μ L buffer D. Alkaline phosphatase substrate was diluted according to kit directions, and 0.1 mL/well was added and developed at room temp for 10 min. The reaction was stopped by adding 0.1 mL 0.4 N NaOH, and the endpoints were read at 405 nm on the V max plate reader. Percent specific binding was calculated by subtracting binding of fibrinogen to BSA-coated wells, and the IC₅₀ values from three replicate experiments were calculated as described above. Notes: In preliminary experiments we determined that fibrinogen binding increased linearly up to 0.3 μ g GP IIB-IIIa added to each well and the addition of higher amounts of GP IIB-IIIa to the wells did not further increase the amount of fibrinogen that bound. Plates coated with GPIIb-IIIa were stored up to 2 months at 4 °C.

Biotinylation of Fibrinogen or Vitronectin. Materials: Purified Fibrinogen (Haematologic Technologies, VT.). Purified Vitronectin 4. Dialysis Buffer: 0.1 M NaHCO₃ pH 8.3, 0.1 M NaCl. TS: 50 mM Tris, pH 7.4, 0.1 M NaCl, 0.05% NaN₃.

Procedure: The ligand (fibrinogen or vitronectin) was dialyzed at 4°C into the dialysis buffer above. In the case of fibrinogen, it was centrifuged in the TL-100 tabletop ultracentrifuge (Beckman Instruments) at 100 000g for 20 min at 4 °C to remove any particulate matter. The ligand concentration was then adjusted to 1 mg/ml with dialysis buffer. Sulfo-N-hydroxysuccinimide-Biotin (Pierce, catalog # 21217) was added as a solid (0.2 mg of biotin ester/mL of ligand) and gently mixed on an end-over-end Nutator for 30 min at room temperature. Unreacted biotin reagent was removed by exhaustive dialysis with TS buffer at 4 °C. The final protein

concentration was determined by O.D. 280 nm (fibrinogen: EC = 1.51 vitronectin: EC = 1.38) and single use aliquots were stored frozen at -80 °C.

HUVEC Adhesion to Vitronectin or Fibronectin. Materials: Human umbilical vein endothelial cells (HUVEC)5. Vitronectin 4 and Fibronectin in PBS. Blocking media: M199 media + 2.5 mg/mL BSA. Assay Media: M199 media + 0.25 mg/mL BSA. 3% paraformaldehyde. 0.5% toluidine blue (dissolved in 3.7% formaldehyde). 2% SDS. Assay controls: Abciximab, an inhibitor of GPIIb-IIIa and the VNR (α v β 3) was purchased from Centocor, Malvern PA; the function blocking fibronectin receptor antibody BIIG2, was a gift from Caroline Damsky6, UCSF; Echistatin, a disintegrin was purchased from Sigma; the cyclic-RGD peptide (C64-89, Mpr-RGDWPC-NH2) was synthesized in house (at COR Therapeutics, Inc.).

Procedure: 1 μ g/well of VN or FN was plated onto Immulon 2 96-well plates and incubated overnight at 4 °C. Before use the plates were washed 2 \times with PBS and blocked for 1-2 h at room temperature. Confluent HUVEC were lifted with trypsin and added to media with serum before pelleting cells. (HUVECs were used between 3rd and ~8th passage). Cells were resuspended in assay media and counted on a hemocytometer. Assay media \pm inhibitors were added to Eppendorf tubes and mixed. Then cells were added such that 100 μ L added to each well yielded ~50 000 cells. The quadruplicate samples were incubated at 37 °C in the 5% CO₂ incubator for 40 min. Nonadherent cells were removed by aspiration and washed 3 \times with 150 μ L PBS. The cells were then fixed by the addition of 100 μ L of 3% paraformaldehyde for 10 min at room temperature. This was aspirated and 90 μ L of 0.5% toluidine blue stained the cells for 3 min. Wells were then washed 2 \times with 150 μ L PBS and 100 μ L 2% SDS was added for 5 min. After mixing well, the plate was read at 650 nm in the Molecular Devices plate reader. Specific adhesion from 2 to 3 separate experiments was determined by subtracting nonspecific HUVEC adhesion to BSA-coated wells from the total.

Assessment of Oral Bioavailability and Other PK Properties in Rats. Sprague Dawley Rats were used for the first assessment of the oral activity of potent compounds. The compounds (double prodrugs, or mono-prodrugs) were solubilized in water and orally administered to six rats. The corresponding free acids were solubilized in 50% PEG-300 and administered intravenously to six rats. The administered doses were 1 mg/kg for all compounds. The animals were instrumented 2 days prior to the experiment and were fully conscious on the day of the experiment. Blood samples were collected on EDTA or sodium citrate and centrifuged to give PPP.

Plasma samples were prepared and extracted using the following method: An internal standard was added to test samples, which were then mixed with an equivalent volume of acetonitrile (ACN) to sediment proteins. The resulting serum was then filtered through a 1000 MW cutoff filter by centrifugation at 5 °C for 1-2 h. Standards were prepared in a plasma and extracted as described above. A 10 point standard curve was prepared for each compound over a concentration range of 5-5000 ng/mL. QC samples, prepared at concentrations of 10, 250, and 2500 ng/mL, were analyzed in triplicate at each concentration. Filtrates were, in some cases, evaporated to dryness, and the residue was dissolved in RP-HPLC mobile phase. In other cases, the UF filtrates were analyzed directly by LC/MS/MS. A variety of LC/MS conditions were used depending on the chromatographic and mass spectral properties of the compounds of interest.

Samples were analyzed for free acids by LC/MS using protocols previously established for these compounds. Individual plasma samples obtained from each rat at each time point following PO dosing were analyzed. For iv administration, composites were prepared of the plasma obtained at each time point and the composites were analyzed (i.e. at each time point, 20 μ L of plasma from each of the rats was mixed to form a composite sample. An aliquot of this composite was analyzed).

Each compound was administered in either a cassette (multiple compounds) form or a single compound form. All drug

administration studies were performed utilizing a serial method of blood sampling. Plasma samples were collected at specific time points, analyzed for plasma concentration, and then reported as mean plasma concentration versus time. The pharmacokinetic profile generated from both treatment groups (orally and intravenously administered) of rats were used to obtain the percent oral bioavailability for each drug. Area under the curve (AUC) data were measured in both groups as well as C_{max} (maximum concentration) and $t_{1/2\beta}$ (half-life). Since the po and iv doses were the same, percent oral bioavailability was simply determined by dividing the AUC in the oral group that received the prodrug by the AUC in the iv group that received the drug (acid form of the compound).

For the in vivo demonstration of GPIIb-IIIa dependence of mouse bleeding time experiment, the compound CT50787 was administered as an iv bolus injection (10% DMSO in water) via tail vein at 10, 40, 50 and 100 mg/kg in approximately 150 μ L volume to anesthetized mice. To initiate bleeding, the tail was transected 2 mm proximal to its tip and immersed in 37 °C normal saline bath. The bleeding time was recorded as the time required until cessation of blood flow or up to 15 min (900 s). PRP of CT50787 in the mouse utilized citrated pooled (C57/Bl) mouse PRP and 20 μ M ADP as the agonist in a standard aggregometry assay.

Pharmacokinetics in Cynomolgus Monkeys. The general procedure for the determination of bioavailability and other pharmacokinetic properties is exemplified here for **27** (CT51269).

The stability of the compounds in rat, cynomolgus monkey, and dog plasmas were evaluated to compare the cholinesterase activities in the various species against the prodrug. Compound stability was also evaluated in a solution containing a suspended section of rat ileum to determine the metabolic stability of the prodrug in the intestine. A standard was used as a control in these studies.

In Vivo Bioavailability. Animals ($n = 3$, weight = 7.1–7.5 kg) were fasted on the afternoon prior to dose administration but water was allowed ad libitum. On the day of the experiment, the monkeys were placed in chair restraints. Blood samples were obtained by percutaneous venipuncture via cephalic or saphenous veins. Blood samples were anticoagulated with EDTA, and the plasma obtained was frozen for later analysis. In the first week of the study, **28** (CT50614) was administered at 200 μ g/kg as a 15 min infusion of the compound dissolved in 50% PEG-300 (2.0 mg/mL) and further diluted with plasmalyte. Each animal received a 3.5 mL infusion of the drug solution for each kg of body weight. In the second week of the study, **27** (CT51269) was dissolved in distilled water at 2.0 mg/mL and administered to the same animals at 2000 μ g/kg via nasogastric feeding tube. An additional 10 mL of water was administered to ensure complete delivery. For intravenously administered compound, blood samples (1.0 mL) were collected at 0 (predose), 5, 15, 30, and 45 min and at 1, 2, 3, 4, 5, 6, 8, 12, 24, 28, 32, and 48 h after dose administration. For orally administered animals, blood samples were collected at 0 (predose), 0.5, 1, 2, 3, 4, 5, 6, 7, 8, 12, 24, 28, 32, and 48 h after dose administration. Blood samples were centrifuged at 1500 g for 10 min, and the resulting platelet poor plasma (PPP) was decanted into Eppendorf tubes and frozen at -15 °C.

Sample Preparation for LC/MS/MS Analysis. A 200 μ L aliquot of the plasma samples was mixed with an equal volume of acetonitrile (ACN), and an internal standard (LY314378) was added to a concentration of 500 ng/mL of plasma. The samples were then centrifuged and filtered through an ultrafiltration membrane (10,000 MW cutoff, Microcon 10, Amicon Inc.). A 60 μ L aliquot of the filtrate was evaporated to dryness in a centrifugal evaporator, and the residue was dissolved in 120 μ L of water containing 0.5% formic acid.

LC/MS/MS Analysis. All separations were performed on a Keystone C18 column (2 \times 10 mm, 5 μ m) using a linear gradient from 5 to 95% ACN over 5 min at a flow rate of 200 μ L/min. Formic acid (0.5%) was used in the mobile phase as an ion-transfer agent for MS detection. The column effluent

was introduced to the MS/MS through a turbo-ion spray source (Temp = 450 °C, ion-spray voltage = 5200 V, turbo-gas flow = 7 L/min). Parent and daughter ions selected for specific MS/MS detection of each compound were used. Collision energies were optimized for maximum sensitivity for each compound, and the optimum settings were used during the scan periods for each compound.

For quantitation, standards of each compound were prepared in cynomolgus monkey plasma and prepared as described above. For each compound, a blank extract was prepared as well as a 10-point standard curve over the concentration range of 1 to 1000 ng/mL. Ratios of peak area of each analyte to that of an internal standard were computed using MacQuan software. Calibration curves were constructed using a weighted ($1/x^2$) linear regression of the standard plasma concentrations to measured peak area ratios. Plasma concentrations of unknowns were determined by interpolation from the corresponding standard curve for each compound.

Quality control samples (QCs) consisting of cynomolgus monkey plasma spiked with either 5, 50, or 500 ng/mL of each compound (three replicates at each concentration) were analyzed with every sample set as a measure of assay performance. Test acceptance criteria required that measured concentrations for QCs be within 20% of theoretical concentrations (accuracy) and that the coefficient of variance for replicate samples at each level be <20% (precision).

In Vitro Determination of Compound Stability in Plasma. Fresh samples of PPP (EDTA anticoagulant) from rat and dog or frozen plasma samples from cynomolgus monkey were used in these experiments. In a typical experiment, compounds were added to plasma (1 mL) to give a final concentration of 2.5 μ g/mL as a DMSO solution (10 μ L of a 250 μ g/mL stock solution). Samples (150 μ L) were taken at 2, 5, 15, 30, 60, and 120 min, mixed with an equal volume of ACN containing an internal standard, centrifuged, and filtered as described above and analyzed by LC/MS/MS. Standards (six-point standard curve) were prepared in either rat or cynomolgus monkey plasma.

In Vitro Metabolism of 27 (CT51269) by Rat Ileum. Freshly harvested intestinal tissue from a single rat was stripped of muscle tissue, blotted dry, cut into two sections (6 \times 6 mm and 7 \times 6 mm), and weighed (27.8 mg and 25.9 mg). The sections were suspended in 2 mL portions of phosphate buffer, and 5 μ g of CT51269 was added to each tube as a DMSO solution (20 μ L of a 250 μ g/mL stock solution). Samples (150 μ L) of the media were taken at 5, 15, 30, 60, and 120 min, mixed with an equal volume of ACN containing an internal standard, centrifuged, and filtered as described above, and analyzed by LC/MS/MS. Standards were prepared in phosphate buffer (six-point standard curve) and treated identically to the samples.

After the 2 h incubation period, 1.25 mL of ACN/IS mixture was added to the sample (consisting of tissue suspended in 1.25 mL of buffer), the sample was homogenized using a sonic probe and mixed for 1 h. The homogenate was centrifuged and filtered using the procedure described above. Analyte concentrations in this sample were determined using a standard curve prepared in phosphate buffer.

LC/MS/MS Determination of Glucuronides of 28 (CT50614) and 29 (CT51270). Two different procedures were used for the determination of glucuronides in the cynomolgus plasma samples. In the first procedure, β -glucuronidase was added to plasma samples obtained from one of the subjects to which **27** (CT51269) had been orally administered. Changes in the concentrations of **28** (CT50614) and **29** (CT51270) were measured by LC/MS/MS relative to similarly treated plasma not treated with glucuronidase. In the second procedure, RP-HPLC effluent was monitored by MS in a narrow mass range around the expected m/z value predicted for CT50614-glucuronide. LC/MS monitoring was also used to verify the extent of hydrolysis of CT50614-glucuronides by the β -glucuronidase treatment.

β -Glucuronidase (100 μ L of a 200 units/mL solution in 8 mM phosphate buffer, Sigma Chemical Co., Cat # G-5897) was

added to 100 μ L of plasma. Control portions of plasma received 100 μ L of phosphate buffer (no enzyme). Both portions were incubated at 37 $^{\circ}$ C for 2 h at which time ACN and an internal standard were added to the sample, and the samples were centrifuged and filtered as described above. Standards (10-point standard curve) and QCs were prepared in cynomolgus PPP and treated identically to the control samples. The concentrations of **27** (CT51269) and **29** (CT51270) were determined using LC/MS/MS as described above.

For direct LC/MS detection of the glucuronide of **28** (CT50614), the control and treated samples were subjected to RP-HPLC as described above. The MS eluant was monitored by MS (Q1 scan) over a scan range of 560–570 amu with a step size of 0.5 amu and a dwell time of 50 ms (total scan time = 1 s).

Pharmacokinetics in Beagle Dogs. The general procedure for the determination of bioavailability and other pharmacokinetic properties is exemplified here for **27** (CT51269).

The pharmacokinetic parameters of **27** (CT51269) were investigated in beagle dogs in a crossover experiment. Plasma samples, collected on EDTA, were analyzed by LC/MS/MS for both the active metabolite of CT51269, **28** (CT50614), and for the inactive, mono-prodrug form of the compound, **29** (CT51270).

Fasted, female beagle dogs (9–10 kg) were used in crossover design studies with a 1 week washout period between studies. In the first week, CT50614 was administered intravenously as an iv bolus in 50% PEG at a dose of 0.1 mg/kg. Blood samples of 1.0 mL were obtained, via percutaneous sampling of the cephalic veins, onto EDTA and centrifuged to give PPP. In the second week, **27** (CT51269) was administered orally, in water, to the same subjects via a 12F feeding tube at a dose of 1 mg/kg.

Plasma samples were analyzed by LC/MS/MS using protocols described above. An internal standard, selected for its chemical similarity to the test compounds, was used in quantitation. The linear range for this assay has been determined to be 1–500 ng/mL with accuracy and precision throughout the range of 85–115% and \pm 10% respectively.

The data were analyzed for pharmacokinetic parameters using WinNonlin software with noncompartmental data treatment.

Acknowledgment. The authors gratefully acknowledge helpful discussions with Charles J. Homcy, David Phillips, and Daniel D. Gretler of Millennium Pharmaceuticals, Inc.

Supporting Information Available: Analytical data, selected HRMS data, tables of 1 H NMR, and HPLC methods/data for final compounds. This material is available free of charge via the Internet at <http://pubs.acs.org>.

References

- (a) Fuster, V.; Badimon, L.; Badimon, J. J.; Chesebro, J. H. The Pathogenesis of Coronary Artery Disease and the Acute Coronary Syndromes (Part I). *N. Engl. J. Med.* **1992**, *326*, 242–250. (b) Fuster, V.; Badimon, L.; Badimon, J. J.; Chesebro, J. H. The Pathogenesis of Coronary Artery Disease and the Acute Coronary Syndromes (Part II). *N. Engl. J. Med.* **1992**, *326*, 310–318. (c) Hynes, R. O. Integrins: Versatility, Modulation, and Signaling in Cell Adhesion. *Cell* **1992**, *69*, 11–25. (d) Humphries, M. J. Integrin Cell Adhesion Receptors and the Concept of Agonism. *Trends Pharmacol. Sci.* **2000**, *21*, 29–32. (e) Aota, S.; Yamada, K. M. Integrin Functions and Signal Transduction. *Adv. Exp. Med. Biol.* **1997**, *400B*, 669–682. (f) Collier, B. S. Blockade of Platelet GPIIb/IIIa Receptors as an Antithrombotic Strategy. *Circulation* **1995**, *92*, 2373–80. (g) Ruef, J.; Katus, H. A. New Antithrombotic Drugs on the Horizon. *Expert Opin. Invest. Drugs* **2003**, *12*(5), 781–797.
- (a) Phillips, D. R.; Charo, I. F.; Parise, L. V.; Fitzgerald, L. A. The Platelet Membrane Glycoprotein IIb-IIIa Complex. *Blood* **1988**, *71*, 831–843.
- (a) Scarborough, R. M.; Naughton, M. A.; Teng, W.; Rose, J. W.; Phillips, D. R.; Nannizzi, L.; Arfsten, A.; Campbell, A. M.; Charo, I. F. Design of Potent and Specific Integrin Antagonists. *J. Biol. Chem.* **1993**, *268*, 1066–1073. (b) Charo, I. F.; Nannizzi, L.; Phillips, D. R.; Hsu, M. A.; Scarborough, R. M. Inhibition of Fibrinogen Binding to GP IIb-IIIa by a GP IIIa Peptide. *J. Biol. Chem.* **1991**, *266*, 1415–1421. (c) Alig, L.; Edenhofer, A.; Hadvary, P.; Hurzeler, M.; Knopp, D.; Muller, M.; Steiner, B.; Trzeciak, A.; Weller, T. Low Molecular Weight, Non-Peptide Fibrinogen Receptor Antagonists. *J. Med. Chem.* **1992**, *35*, 4393–4407. (d) Zablocki, J. A.; Miyano, M.; Garland, R. B.; Pireh, D.; Schretzman, L. A.; Rao, S. N.; Lindmark, R. J.; Panzer-Knodle, S. G.; Nicholson, N. S.; Taite, B. B.; Salyers, A. K.; King, L. W.; Campion, J. G.; Feigen, L. P. Potent in Vitro and in Vivo Inhibitors of Platelet Aggregation Based upon the Arg-Gly-Asp-Phe Sequence of Fibrinogen: A Proposal on the Nature of the Binding Interaction between the Arg-guanidine of RGDx Mimetics and the Platelet GP IIb-IIIa Receptor. *J. Med. Chem.* **1993**, *36*, 1811–1819.
- (a) Lincoff, A. M.; Topol, E. J. Overview of the Glycoprotein IIb/IIIa Interventional Trials. In *Platelet Glycoprotein IIb/IIIa Inhibitors in Cardiovascular Disease*, 2nd ed.; Lincoff, A., Michael, Eds.; Humana Press Inc.: Totowa, N. J., 2003; pp 167–199. (b) Agah, R.; Plow, E. F.; Topol, E. J. GPIIb-IIIa Antagonists. In *Platelets*; Michelson, A. D., Eds.; Academic Press: California, 2002; pp 769–785.
- Lincoff, A. M.; Califf, R. M.; Topol, E. J. Platelet Glycoprotein IIb-IIIa Receptor Blockade in Coronary Artery Disease. *J. Am. Coll. Cardiol.* **2000**, *35*, 1103–1115.
- (a) Collier, B. S. Anti-GPIIb/IIIa Drugs: Current Strategies and Future Directions. *Thromb. Haemost.* **2001**, *86*, 427–443. (b) Konstantopoulos, K.; Mousa, S. A. Antiplatelet Therapies: Platelet GPIIb/IIIa Antagonists and Beyond. *Curr. Opin. Invest. Drugs* **2001**, *2*, 1086–1092. (c) Dogne, J.; De Leval, X.; Benoit, P.; Delarge, J.; Masereel, B.; David, J. Recent advances in antiplatelet agents. *Curr. Med. Chem.* **2002**, *9*, 577–589. (d) Ojima, I.; Chakravarty, S.; Dong, Q. Antithrombotic Agents: From RGD to Peptide Mimetics. *Bioorg. Med. Chem.* **1995**, *3*, 337–360. (e) Scarborough, R. M. Structure–Activity Relationships of β -Amino Acid-Containing Integrin Anagonists. *Curr. Med. Chem.* **1999**, *6*, 971–981.
- Mousa, S. A.; Iqbal, O.; Fareed, J. Antithrombotics and Thrombolytics in Stroke. *Curr. Opin. Invest. Drugs* **2002**, *3*, 878–885.
- Wang, W.; Borchardt, R. T.; Wang, B. Orally Active Peptidomimetic RGD Analogues that are Glycoprotein IIb/IIIa Antagonists. *Curr. Med. Chem.* **2000**, *7*, 437–453.
- (a) Cannon, C. P. The Evolving Story of Oral Platelet Glycoprotein IIb-IIIa Receptor Inhibitors. *Curr. Opin. Cardiovascular, Pulmonary & Renal Invest. Drugs* **2000**, *2*, 114–123. (b) Quinn, M. J.; Plow, E. F.; Topol, E. J. Platelet Glycoprotein IIb/IIIa Inhibitors: Recognition of a Two-Edged Sword? *Circulation* **2002**, *106*, 379–385.
- Scarborough, R. M. Eptifibatid. *Drugs Future* **1998**, *23*(6), 585–590.
- Scarborough, R. M.; Gretler, D. D. Platelet Glycoprotein IIb-IIIa Antagonists as Prototypical Integrin Blockers: Novel Parenteral and Potential Oral Antithrombotic Agents. *J. Med. Chem.* **2000**, *43*(19), 3453–3473.
- (a) Scarborough, R. M.; Kleiman, N. S.; Phillips, D. R. Platelet Glycoprotein IIb/IIIa Antagonists: What Are the Relevant Issues Concerning their Pharmacology and Clinical Use? *Circulation* **1999**, *100*, 437–444. (b) Brassard, J. A.; Curtis, B. R.; Cooper, R. A.; Ferguson, J.; Komocsar, W.; Ehardt, M.; Kupfer, S.; Maurath, C.; Swabb, E.; Cannon, C. P.; Aster, R. H. Acute Thrombocytopenia in Patients Treated with the Oral Glycoprotein IIb/IIIa Inhibitors Xemilofiban and Orbofiban: Evidence for an Immune Etiology. *Thromb. Haemost.* **2002**, *88*, 892–897. (c) Aster, R. H. Thrombocytopenia Induced by GPIIb/IIIa Inhibitors. *Blood* **2003**, *101*, 1. (d) Peter, K.; Schwarz, M.; Nordt, T.; Bode, C. Intrinsic Activating Properties of GP IIb/IIIa Blockers. *Thromb. Res.* **2001**, *103* (Suppl. 1), S21–S27. (e) Iqbal, O.; Walenga, J. M.; Lewis, B. E.; Bakhos, M. Bleeding Complications with Glycoprotein IIb/IIIa Inhibitors. *Drugs Today* **2000**, *36*, 503–514. (f) Billheimer, J. T.; He, B.; Spitz, S. M.; Stern, A. M.; Seiffert, D. Effects of Glycoprotein IIb/IIIa Antagonists on Platelet Activation: Development of a Transfer Method to Mimic Peak to Trough Receptor Occupancy. *Thromb. Res.* **2002**, *107* (6), 303–317.
- (a) Salam, A. M.; Al Suwaidi, J. Platelet Glycoprotein IIb/IIIa Antagonists in Clinical Trials for the Treatment of Coronary Artery Disease. *Exp. Opin. Invest. Drugs* **2002**, *11*, 1645–1658. (b) Peter, K.; Straub, A.; Kohler, B.; Volkmann, M.; Schwarz, M.; Kubler, W.; Bode, C. Platelet Activation as a Potential Mechanism of GP IIb/IIIa Inhibitor-Induced Thrombocytopenia. *Am. J. Cardiol.* **1999**, *84*, 519–524.
- (a) Hosking, M. P.; Carroll, R. C. Roxifiban, DuPont. *Curr. Opin. Cardiovasc. Pulm. Renal Invest. Drugs* **2000**, *2*, 165–171. (b) Mousa, S. A.; Bozarth, J. M.; Naik, U. P.; Slee, A. Platelet GPIIb/IIIa Binding Characteristics of Small Molecule RGD Mimetic: Distinct Binding Profile for Roxifiban. *Br. J. Pharmacol.* **2001**, *133*, 331–336. (c) Mousa, S. A.; Kapil, R.; Mu, D. Intravenous and Oral Antithrombotic Efficacy of the Novel Platelet GPIIb/IIIa Antagonist Roxifiban (DMP754) and its Free Acid Form, XV459. *Arterioscler. Thromb. Vasc. Biol.* **1999**, *19*, 2535–2541.

- (d) Gurbel, P. A.; McKenzie, M. E.; Serebruany, V. L. Initial Platelet Activity may Predict Efficacy after Chronic Oral Glycoprotein IIb/IIIa Blockade: Should We Still Consider Uniform Treatment Regimens? *Thromb. Res.* **2000**, *99*, 105–107. (e) Fossler, M. J.; Ebling, W. F.; Ma, S.; Kornhauser, D.; Mondick, J.; Barrett, J. S.; Garner, D.; Quon, C. Y.; Pieniaszek, H. J., Jr. Integrated Pharmacokinetic/Pharmacodynamic Model of XV459, a Potent and Specific GPIIb/IIIa Inhibitor, in Healthy Male Volunteers. *J. Clin. Pharmacol.* **2002**, *42*, 1326–1334.
- (15) (a) Smyth, M. S.; Rose, J.; Mehrotra, M. M.; Heath, J.; Ruhter, G.; Schotten, T.; Seroogy, J.; Volkots, D.; Pandey, A.; Scarborough, R. M. Spirocyclic Nonpeptide Glycoprotein IIb-IIIa Antagonists. Part 1: Design of Potent and Specific 3,9-Diazaspiro[5.5]undecanes. *Bioorg. Med. Chem. Lett.* **2001**, *11*, 1289–1292. (b) Pandey, A.; Seroogy, J.; Volkots, D.; Smyth, M. S.; Rose, J.; Mehrotra, M. M.; Heath, J.; Ruhter, G.; Schotten, T.; Scarborough, R. M. Spirocyclic Nonpeptide Glycoprotein IIb-IIIa Antagonists. Part 2: Design of Potent Antagonists Containing the 3-Azaspiro[5.5]undec-9-yl Template. *Bioorg. Med. Chem. Lett.* **2001**, *11*, 1293–1296. (c) Mehrotra, M. M.; Heath, J.; Rose, J.; Smyth, M. S.; Seroogy, J.; Volkots, D.; Ruhter, G.; Schotten, T.; Alaimo, L.; Park, G.; Pandey, A.; Scarborough, R. M. Spirocyclic Nonpeptide Glycoprotein IIb-IIIa Antagonists. Part 3: Synthesis and SAR of Potent and Specific 2,8-Diazaspiro[4.5]decanes. *Bioorg. Med. Chem. Lett.* **2002**, *12*, 1103–1107. (d) Fisher, M. J.; Jakubowski, J. A.; Masters, J. J.; Mullaney, J. T.; Ruterbories, K. J.; Paal, M.; Ruhter, G.; Scarborough, R. M.; Schotten, T.; Stenzel, W. Spiro Compounds as Inhibitors of Fibrinogen-Dependent Platelet Aggregation. U.S. Patent 6291469, 2001.
- (16) (a) Wagner, G.; Voigt, B.; Vieweg, H. Synthesis of N- α -(Arylsulfonyl)glycyl) amidinophenylalaninamides as Highly Active Inhibitors of Thrombin. *Pharmazie* **1984**, *39*, 226–230. (b) Judkins, B. D.; Allen, D. G.; Cook, T. A.; Evans, B.; Sardharwala, T. E. A Versatile Synthesis of Amidines from Nitriles Via Amidoximes. *Synth. Commun.* **1996**, *26*(23), 4351–4367.
- (17) (a) Rawal, V. H.; Jones, R. J.; Cava, M. P. Photocyclization Strategy for the Synthesis of Antitumor Agent CC-1065: Synthesis of Dideoxy PDE-I and PDE-II. Synthesis of Thiopene and Furan Analogues of Dideoxy PDE-I and PDE-II. *J. Org. Chem.* **1987**, *52*, 19–28. (b) Reinecke, M. G.; Daubert, R. G. Peripheral Synthesis of Secondary Medium-Ring Nitrogen Heterocycles. *J. Org. Chem.* **1973**, *38*, 3281–3287.
- (18) Dong, Q.; Anderson, C. E.; Ciufolini, M. A. Reductive Cleavage of TROC Groups under Neutral Conditions with Cadmium-Lead Couple. *Tetrahedron Lett.* **1995**, 5681–5682.
- (19) (a) Carrera, G. M., Jr.; Garvey, D. S. Synthesis of Novel Substituted Spirohydantoin. *J. Heterocycl. Chem.* **1992**, *29*, 847–850. (b) Suess, R. Substituierte 2,8-Diazaspiro-decan-1,3-dione. *Helv. Chim. Acta* **1977**, *60*(5), 1650–1656; & Jucker, E.; Sue, R. *Arch. Pharm.* **1961**, *294*, 210–220.
- (20) Fisher, M. J.; Gunn, B.; Harms, C. S.; Kline, A. D.; Mullaney, J. T.; Nunes, A.; Scarborough, R. M.; Arfsten, A. E.; Skelton, M. A.; Um, S. L.; Utterback, B. G.; Jakubowski, J. A. Non-Peptide RGD Surrogates which Mimic a Gly-Asp β -Turn: Potent Antagonists of Platelet Glycoprotein IIb-IIIa. *J. Med. Chem.* **1997**, *40*, 2085–2101.
- (21) Su, T.; Naughton, M. A.; Smyth, M. S.; Rose, J. W.; Arfsten, A. E.; McCowan, J. R.; Jakubowski, J. A.; Wyss, V. L.; Ruterbories, K. J.; Sall, D. J.; Scarborough, R. M. Fibrinogen Receptor (GPIIb/IIIa) Antagonists Derived from 5,6-Bicyclic Templates. Amidinoindoles, Amidinoindazoles, and Amidinobenzofurans Containing the N- α -Sulfonamide Carboxylic Acid Function as Potent Platelet Aggregation Inhibitors. *J. Med. Chem.* **1997**, *40*, 4308–4318.
- (22) (a) Hartman, G. D.; Egbertson, M. S.; Halczenko, W.; Laswell, W. L.; Duggan, M. E.; Smith, R. L.; Naylor, A. M.; Manno, P. D.; Lynch, R. J.; Zhang, G.; Chang, C. T.-C.; Gould, R. J. Non-Peptide Fibrinogen Receptor Antagonists. 1. Discovery and Design of Exosite Inhibitors. *J. Med. Chem.* **1992**, *35*, 4640–4642. (b) Egbertson, M. S.; Chang, C. T.-C.; Duggan, M. E.; Gould, R. J.; Halczenko, W.; Hartman, G. D.; Laswell, W. L.; Lynch, Jr. J. J.; Lynch, R. J.; Manno, P. D.; Naylor, A. M.; Prugh, J. D.; Ramjit, D. R.; Sitko, G. R.; Smith, R. S.; Turchi, L. M.; Zhang, G. Non-Peptide Fibrinogen Receptor Antagonists. 2. Optimization of a Tyrosine Template as a Mimic for Arg-Gly-Asp. *J. Med. Chem.* **1994**, *37*, 2537–2551. (c) Xue, C.-B.; Roderick, J.; Jackson, S.; Rafalski, M.; Rockwell, A.; Mousa, S.; Olson, R. E.; DeGrado, W. F. Design, Synthesis, and in Vitro Activities of Benzamide-Core Glycoprotein IIb-IIIa Antagonists: 2,3-Diaminopropionic Acid Derivatives as Surrogates of Aspartic Acid. *Bioorg. Med. Chem.* **1997**, *5*, 693–705.
- (23) (a) Scarborough, R. M.; Rose, J. W.; Naughton, M. A.; Phillips, D. R.; Namizzi, L.; Arfsten, A.; Campbell, A. M.; Charo, I. F. Characterization of the Integrin Specificities of Disintegrins Isolated from American Pit Viper Venoms. *J. Biol. Chem.* **1993**, *268*, 1058–1065. (b) Duggan, M. E.; Naylor-Olsen, A. M.; Perkins, J. J.; Anderson, P. S.; Chang, C. T.-C.; Cook, J. J.; Gould, R. J.; Ihle, N. C.; Hartman, G. D.; Lynch, J. J.; Lynch, R. J.; Manno, P. D.; Schaffer, L. W.; Smith, R. L. Non-Peptide Fibrinogen Receptor Antagonists. 7. Design and Synthesis of a Potent, Orally Active Fibrinogen Receptor Antagonist. *J. Med. Chem.* **1995**, *38*, 3332–3341.
- (24) Zablocki, J. A.; Rico, J. G.; Garland, R. B.; Rogers, T. E.; Williams, K.; Schretzman, L. A.; Rao, S. A.; Bovy, P. R.; Tjoeng, F. S.; Lindmark, R. J.; Toth, M. V.; Zupec, M. E.; McMackins, D. E.; Adams, S. P.; Miyano, M.; Markos, C. S.; Milton, M. N.; Paulson, S.; Herin, M.; Jacqmin, P.; Nicholson, N. S.; Panzer-Knodle, S. G.; Haas, N. F.; Page, J. D.; Szalony, J. A.; Taite, B. B.; Salyers, A. K.; King, L. W.; Campion, J. G.; Feigen, L. P. Potent in vitro and in vivo Inhibitors of Platelet Aggregation Based upon the Arg-Gly-Asp Sequence of Fibrinogen. (Aminobenzamidino)succinyl (ABAS) Series of Orally Active Fibrinogen Receptor Antagonists. *J. Med. Chem.* **1995**, *38*, 2378–2394.
- (25) Mills, S. D. Heterocyclic Compounds. U.S. Patent 5,753,659, 1998.
- (26) Samanen, J. M.; Ali, F. E.; Barton, L. S.; Bondinell, W. E.; Burgess, J. L.; Callahan, J. F.; Calvo, R. R.; Chen, W.; Chen, L.; Erhard, K.; Feuarstein, G.; Heys, R.; Hwang, S.-M.; Jckas, D. R.; Keenan, R. M.; Ku, T. W.; Kwon, C.; Lee, C.-P.; Miller, W. H.; Newlander, K. A.; Nichols, A.; Parker, M.; Peishoff, C. E.; Rhodes, G.; Ross, S.; Shu, A.; Simpson, R.; Takata, D.; Yellin, T. O.; Uzsinskas, I.; Vensalavsky, J. W.; Yuan, C.-K.; Huffman, W. F. Potent, Selective, Orally Active 3-Oxo-1,4-benzodiazepine GPIIb-IIIa Integrin Antagonists. *J. Med. Chem.* **1996**, *39*, 4867–4870.
- (27) Damiano, B. P.; Mitchell, J. A.; Giardino, E.; Corcoran, T.; Haertlein, B. J.; De Garavilla, L.; Kauffman, J. A.; Hoekstra, W. J.; Maryanoff, B. E.; Andrade-Gordon, P. Antiplatelet and Antithrombotic Activity of RWJ-53308, a Novel Orally Active Glycoprotein IIb/IIIa Antagonist. *Thromb. Res.* **2001**, *104*, 113–126.
- (28) (a) Hayashi, Y.; Katada, J.; Harada, T.; Tachki, A.; Iijima, K.; Takiguchi, Y.; Muramatsu, M.; Miyazaki, H.; Asari, T.; Okazaki, T.; Sato, Y.; Yasuda, E.; Yano, M.; Uno, I.; Ojima, I. GPIIb-IIIa Integrin Antagonists with the New Conformational Restriction Unit, Trisubstituted β -Amino Acid Derivatives, and a Substituted Benzamide Structure. *J. Med. Chem.* **1998**, *41*, 2345–2360. (b) Okumura, K.; Shimazaki, T.; Aoki, Y.; Yamashita, H.; Tanaka, E.; Banba, S.; Yazawa, K.; Kibayashi, K.; Banno, H. New Platelet Fibrinogen Receptor Glycoprotein IIb-IIIa Antagonists: Orally Active Series of N-Alkylated Amidines with a 6,6-Bicyclic Template. *J. Med. Chem.* **1998**, *41*, 4036–4052. (c) Yamashita, H.; Okumura, K.; Shimazaki, T.; Kanematsu, A.; Aoki, Y.; Nakajima, Y.; Yazawa, K.; Kibayashi, K. Amidine Derivatives and Platelet Aggregation Inhibitor Containing the Same. European Patent 0760364A2, 1997.
- (29) Muller, T. H.; Schurer, H.; Waldmann, L.; Bauer, E.; Himmelsbach, F.; Binder, K. Oral Activity of BIBU 104, a Prodrug of the Non-Peptide Fibrinogen Receptor Antagonist BIBU 52, in Mice and Monkeys. *Thromb. Haemostasis* **1993**, *69*, 975, Abstract 1557.
- (30) (a) Merlos, M.; Graul, A.; Castaner, J. Sibrafilan *Drugs Future* **1998**, *23*, 1297–1303. (b) Weller, T.; Alig, L.; Beresini, M.; Blackburn, B.; Bunting, S.; Hadvary, P.; Muller, M. H.; Knopp, D.; Levet-Trafit, B.; Lipari, M. T.; Modi, N. B.; Muller, M.; Refino, C. J.; Schmitt, M.; Schonholzer, P.; Weiss, S.; Steiner, B. Orally Active Fibrinogen Receptor Antagonists. 2. Amidoximes as Prodrugs of Amidines. *J. Med. Chem.* **1996**, *39*, 3139–3147.
- (31) Gante, J.; Juraszyk, H.; Raddatz, P.; Wurziger, H.; Bernotat-Danielowski, S.; Melzer, G.; Rippmann, F. New Antithrombotic RGD-Mimetics with High Bioavailability. *Bioorg. Med. Chem. Lett.* **1996**, *6* (20), 2425–2430.
- (32) Veber, D. F.; Johnson, S. R.; Cheng, H.-Y.; Smith, B. R.; Ward, K. W.; Kopple, K. D. Molecular Properties that Influence the Oral Bioavailability of Drug Candidates. *J. Med. Chem.* **2002**, *45*, 2615–2623.
- (33) (a) Hauptmann, J.; Paintz, M.; Kaiser, B.; Richter, M. Reduction of a Benzamidoxime Derivative to the Corresponding Benzamide in Vivo and in Vitro. *Pharmazie* **1988**, *43*, 559–560. (b) Clement, B.; Zimmermann, M.; Schmitt, S. Biotransformation des Benzamidins und des Benzamidoxims durch mikrosomale Enzyme vom Kaninchen. (Biotransformation of Benzamide and Benzamidoxime by Microsomal Enzymes of the Rabbit.) *Arch. Pharm. (Weinheim, Ger.)* **1989**, *322*, 431–435. (c) Clement, B.; Immel, M.; Terlinden, R.; Wingen, F.-J. Reduction of Amidoxime Derivatives to Pentamide in vivo. *Arch. Pharm. (Weinheim, Ger.)* **1992**, *325*, 61–62. (d) Clement, B.; Jung, F. N-Hydroxylation of the Antiprotazoal Drug Pentamide Catalyzed by Rabbit Liver Cytochrome P-450 2C3 or Human Liver Microsomes, Microsomal Retroreduction, and Further Oxidative Transformation of the Formed Amidoximes. *Drug Metab. Dispos.* **1994**, *22*, 486–497.

- (34) Ertl, P.; Rohde, B.; Selzer, P. Fast Calculation of Molecular Polar Surface Area as a Sum of Fragment-Based Contributions and its Application to the Prediction of Drug Transport Properties. *J. Med. Chem.* **2000**, *43*, 3714–3717.
- (35) We have recently reported that when **22** (CT51464/ML464) was administered to mice by oral gavage at a dose of 100 mg/kg, platelet aggregation, measured by platelet-rich plasma aggregation, was inhibited within 30 min and remained disrupted for up to 10 h. During this time, the concentration of active

metabolite **23** (CT50728/ML728) was 37.5 μ M at its peak 30 min after oral gavage and 5 μ M 8 h after oral gavage of **22**. Bakewell, S. J.; Nester, P.; Prasad, S.; Tomasson, M. H.; Dowland, N.; Mehrotra, M.; Scarborough, R.; Kanter, J.; Abe, K.; Phillips, D.; Weilbaeher, K. N. Platelet and Osteoclast β_3 Integrins are Critical for Bone Metastasis. *Proc. Natl. Acad. Sci. U.S.A.* **2003**, *100* (24), 14205–14210.

JM030354B